

RADC-TR-81-13
Final Technical Report
March 1981

LEVEL II

12



AD A 098105

ANALYSIS OF ADVANCED CI APPLICATIONS

Optical Sciences Company

Sponsored by
Defense Advanced Research Projects Agency (DoD)
ARPA Order No. 2646

DTIC
ELECTE
S APR 23 1981 D
E

APPROVED FOR PUBLIC RELEASE; DISTRIBUTION UNLIMITED

The views and conclusions contained in this document are those of the authors and should not be interpreted as necessarily representing the official policies, either expressed or implied, of the Defense Advanced Research Projects Agency or the U. S. Government.

ROME AIR DEVELOPMENT CENTER
Air Force Systems Command
Griffiss Air Force Base, New York 13441

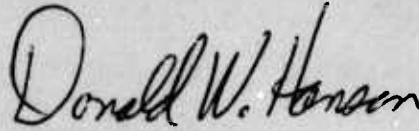
DTIC FILE COPY

81 4 23 040

This report has been reviewed by the RADC Public Affairs Office (PA) and is releasable to the National Technical Information Service (NTIS). At NTIS it will be releasable to the general public, including foreign nations.

RADC-TR-81-13 has been reviewed and is approved for publication.

APPROVED:



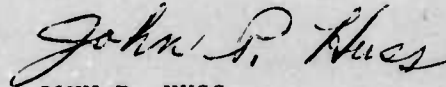
DONALD W. HANSON
Project Engineer

APPROVED:



FRANK J. REHM
Technical Director
Surveillance Division

FOR THE COMMANDER:



JOHN P. HUSS
Acting Chief, Plans Office

If your address has changed or if you wish to be removed from the RADC mailing list, or if the addressee is no longer employed by your organization, please notify RADC (OCSE) Griffiss AFB NY 13441. This will assist us in maintaining a current mailing list.

Do not return this copy. Retain or destroy.

ANALYSIS OF ADVANCED CI APPLICATIONS

David L. Fried

Contractor: Optical Sciences Company
Contract Number: F30602-79-C-0062
Effective Date of Contract: 20 March 1979
Contract Expiration Date: 30 September 1980
Short Title of Work: Analysis of Advanced CI
Applications
Program Code Number: OE20
Period of Work Covered: Apr 80 - Oct 80
Principal Investigator: Dr. David L. Fried
Phone: 714 524-3622
Project Engineer: Donald W. Hanson
Phone: 315 330-3145

Approved for public release; distribution unlimited.

This research was supported by the Defense Advanced Research Projects Agency of the Department of Defense and was monitored by Donald W. Hanson (OCSE), Griffiss AFB NY 13441 under Contract F30602-79-C-0062.

UNCLASSIFIED

SECURITY CLASSIFICATION OF THIS PAGE (When Data Entered)

READ INSTRUCTIONS BEFORE COMPLETING FORM

19 REPORT DOCUMENTATION PAGE		3. RECIPIENT'S CATALOG NUMBER	
1. REPORT NUMBER	2. GOVT ACCESSION NO.	AD-A098105	
18 RADC-TR-81-13	4. TITLE (and Subtitle)		
6 ANALYSIS OF ADVANCED CI APPLICATIONS	9	5. TYPE OF REPORT & PERIOD COVERED	
	14	Final Technical Report Apr 80 - Oct 80	
	10	6. PERFORMING ORG. REPORT NUMBER	
		7. CONTRACT OR GRANT NUMBER(s)	
		F30602-79-C-0062 WARPA Order-2646	
8. AUTHOR(s)		10. PROGRAM ELEMENT PROJECT TASK AREA & WORK UNIT NUMBERS	
David L. Fried		62301E 26460411 17/14	
9. PERFORMING ORGANIZATION NAME AND ADDRESS		12. REPORT DATE	
Optical Sciences Co P O Box 446 Placentia CA 92670		March 1981	
11. CONTROLLING OFFICE NAME AND ADDRESS		13. NUMBER OF PAGES	
Defense Advanced Research Projects Agency 1400 Wilson Blvd Arlington VA 22209		64	
14. MONITORING AGENCY NAME & ADDRESS (if different from Controlling Office)		15. SECURITY CLASS. (of this report)	
Rome Air Development Center (OCSE) Griffiss AFB NY 13441		UNCLASSIFIED	
16. DISTRIBUTION STATEMENT (of this Report)		15a. DECLASSIFICATION/DOWNGRAIDING SCHEDULE	
Approved for public release; distribution unlimited.		N/A	
17. DISTRIBUTION STATEMENT (of the abstract entered in Block 20, if different from Report)			
Same			
18. SUPPLEMENTARY NOTES			
RADC Project Engineer: Donald W. Hanson (OCSE)			
19. KEY WORDS (Continue on reverse side if necessary and identify by block number)			
Atmospheric Optics. Compensated Imaging Turbulence Uplink Adaptive Optics Laser Transmitter			
20. ABSTRACT (Continue on reverse side if necessary and identify by block number)			
This report is the last of three technical reports prepared on this contract. It treats two subjects. In Chapter 1 the first subject, the effect of daylight background on CIS operation, is analyzed. It is concluded that such operation should be feasible and yield acceptable performance for all but the faintest targets of nominal interest to the CIS. The analysis is concerned with shot noise limits and assumes that all matters that could be classified as alignment or adjustment of the			

DD FORM 1 JAN 73 1473

EDITION OF 1 NOV 65 IS OBSOLETE

UNCLASSIFIED

SECURITY CLASSIFICATION OF THIS PAGE (When Data Entered)

391 358

Handwritten initials and a checkmark.

UNCLASSIFIED

SECURITY CLASSIFICATION OF THIS PAGE(When Data Entered)

system have been properly aligned or adjusted. The second subject is treated in Chapter 2, and is concerned with the definition of a practical form for an UpLink adaptive optics laser transmitter experiment. The critical features of a ground to aircraft and a ground to space experiment are identified, implementation approaches are suggested, and magnitude of relevant parameters are determined.

UNCLASSIFIED

SECURITY CLASSIFICATION OF THIS PAGE(When Data Entered)

TABLE OF CONTENTS

<u>Chapter</u>	<u>Section</u>	<u>Title</u>	<u>Page</u>
I		Feasibility of CIS Operation During Daylight Hours	1
	1.	Introduction to Chapter I	2
	1.2	Photon Flux Ratios	4
	1.3	System Performance Degradation	11
	1.4	References for Chapter I	15
II		Configuration and Analysis for an UpLink Experiment/Demonstration	16
	2.1	Introduction to Chapter II	17
	2.2	General Considerations	18
	2.3	Experiment Description	21
	2.3.1	Aircraft Experiment	22
	2.3.2	Satellite Experiment	29
	2.4	Numerical Considerations	35
	2.4.1	Propagation Effects	35
	2.4.2	Point Ahead	46
	2.4.3	Beacon Power	49
	2.5	Conclusions and Summary for Chapter II	56

Accession For	
NTIS GRA&I	<input checked="" type="checkbox"/>
DTIC TAB	<input type="checkbox"/>
Unannounced	<input type="checkbox"/>
Justification	
By _____	
Distribution/	
Availability Codes	
Dist	Avail and/or Special
A	

LIST OF FIGURES

<u>Figure No.</u>	<u>Title</u>	<u>Page</u>
1	Spectral distribution of diffuse radiation with clear skies at the zenith (1) and at a point where the sky luminance is minimal (2).	5
2	Energy distribution in the solar spectrum outside the atmosphere.	5
3	Effective Coherence Diameter.	38
4	Greenwood Frequency.	39
5	Angular Extent of the Isoplantic Patch.	40
6	Linear Extent of the Isoplantic Patch.	40
7	Log-Amplitude Variance.	43

LIST OF TABLES

<u>Table No.</u>	<u>Title</u>	<u>Page</u>
1	Model clear sky luminance distribution (cd/m^2) for a solar elevation $\pi/4$ rads, azimuth 0 rads.	6
2a	Background to Target Ratio, \mathfrak{R} , for Sky Brightness, B, Equal to 1000 lumens/ m^2 -ster.	8
2b	Background to Target Ratio, \mathfrak{R} , for Sky Brightness, B, Equal to 6000 lumens/ m^2 -ster.	9
3a	Equivalent Target Brightness, \tilde{m}_{RE} , for Sky Brightness, B, Equal to 1000 lumens/ m^2 -ster.	13
3b	Equivalent Target Brightness, \tilde{m}_{RE} , for Sky Brightness, B, Equal to 6000 lumens/ m^2 -ster.	14

Chapter I

Feasibility of CIS Operation

During Daylight Hours

1. Introduction to Chapter I

The compensated imaging system being built by Itek has been designed for night time operation. Nonetheless, the possibility exists that the system will be able to operate during daylight hours, if the target is bright enough. In the first order examination of this problem, which we conduct in this chapter, the feasibility of daylight operation hinges on the excess shot noise produced by the greater background brightness and whether or not this is large enough to overwhelm the target signal. Eventually there has to be consideration of more subtle matters, such as whether the background photon flux rate would be so high as to saturate the photon detection/counting system, or whether it will be possible to adjust/hold the field-of-view stop setting with sufficient precision that the background chopping noise will not significantly affect the measured phase of the chopped target signal. However, such, more subtle matter will not be considered here. Instead we shall restrict our attention to the dominant question of whether or not there is sufficient signal-to-noise ratio available with the daylight background present, to allow meaningful system operation even if everything is otherwise adequately sized.

The basic compensated imaging system, as developed for nighttime operation derives its noise limit from the photon shot-noise inherent in the target signal. It is therefore sufficient for our purpose to simply concern ourselves with the ratio of the daylight sky background photons to the target photons. So long as the sky background photon flux rate is the smaller there will be no significant degradation of system performance. However, to the extent that it is larger, the signal-to-noise ratio situation will be degraded and system performance will be reduced.

One rather surprising implication of the situation with daylight background operation pertains to the dependence on target size. We know

that for night time operation, so long as the target is resolvable, system performance does not depend on target size. Performance is determined by brightness per resolution element, and is otherwise independent of total target brightness (which is a function of brightness per resolution element and of target size). However, when the system is operating in the daytime we need to ask about the ratio of the background flux to the target signal photon flux, and this ratio does depend on target size, i. e. , on total brightness and not just on brightness per resolution element. When the noise is due to the target signal flux, i. e. , for night time operation, increasing the target size and the total photon flux, only increases the useful signal amplitude as much as it increases the rms noise, so that making the target larger does not improve the effective signal-to-noise ratio. On the other hand, for daytime operation, when the sky background is producing a greater photon flux than the target, then increasing the target size will increase the useful signal amplitude, but will have only a negligible effect on the total photon flux, and thus only a negligible effect on the rms noise. Thus increasing the target size will, for daytime operation, improve the effective signal-to-noise ratio and the compensated imaging system's performance.

To put the matter of daytime operation of the compensated imaging system on a quantitative basis, in the next section we shall develop some ratios for target-to-sky background photon flux. In the section after that we shall develop some scaling laws for the effect of various ratio values on the performance of the compensated imaging system.

1.2 Photon Flux Ratios

In this section we shall be concerned with the task of developing an expression for the ratio, \mathcal{R} , of the daytime sky background flux, \mathcal{B} , to the target flux, \mathcal{I} ,

$$\mathcal{R} = \mathcal{B} / \mathcal{I} \quad . \quad (1)$$

For convenience, because our starting data is basically available in luminance units (i. e., lumens/m² and lumens/m²-ster), we shall calculate \mathcal{B} and \mathcal{I} in luminance units. To the extent that the compensated imaging system's adaptive optics sensors have a responsivity curve like that of the eye, use of luminosity units will provide a valid basis for comparison, and \mathcal{R} , as defined by Eq. (1) will be a directly meaningful number. Because of the difference between the spectral distribution of sky brightness as shown in Fig. 1, and that of the target brightness (corresponding to that of the incident solar spectrum), which is shown in Fig. 2, we may expect that a comparison of luminosity values will not exactly represent the situation if the sensor's responsivity is not exactly proportional to luminosity. For the purposes of this analysis, however, it is reasonable to expect that such an effect will be sufficiently minor that we can ignore it here—and accordingly, will carry out our calculations in luminosity units.

The sky background flux, \mathcal{B} , measured in lumens, can be written as

$$\mathcal{B} = B \theta (48.5 \times 10^{-6}) A \quad , \quad (2)$$

where B is the sky brightness (in units of lumens/m²-ster), θ is the width of the sensor field-of-view (in units of radians), 48.5×10^{-6} radians is the nominal length of the sensor field-of-view (corresponding to ten arc-seconds), and A is the telescope's effective aperture area. The magnitude of the sky

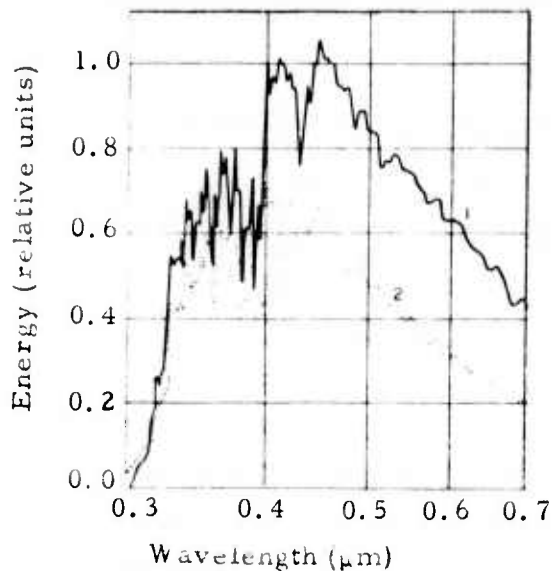


Figure 1. Spectral distribution of diffuse radiation with clear skies at the zenith (1) and at a point where the sky luminance is minimal (2).
Nach Kondratyev¹

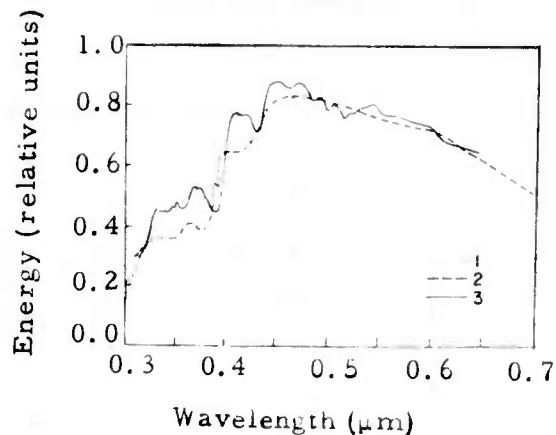


Figure 2. Energy distribution in the solar spectrum outside the atmosphere.
Nach Kondratyev²

brightness, B , depends on the zenith angle of the line-of-sight and on the position relative to the sun. In Table 1 we show some sample values of B . Restricting attention to zenith angles of 60° or less, and avoiding the region of sky within 45° of the sun, the relevant range of values of B run from about $1000 \text{ lumens/m}^2\text{-ster}$ to about $6000 \text{ lumens/m}^2\text{-ster}$, i. e.,

$$1000 < B < 6000 \quad \text{lumens/m}^2\text{-ster} . \quad (3)$$

The value of θ , the width of the field-of-view will be larger than the target's angular diameter, θ_T , and recognizing isoplanatism problems need never be any greater than 48.5×10^{-6} radians (i. e., ten arc seconds). Thus, we can write

$$\theta_T < \theta < 48.5 \times 10^{-6} \text{ radians} . \quad (4)$$

Table 1. Model clear sky luminance distribution (cd/m^2)* for a solar elevation $\pi/4$ rads, azimuth 0 rads. From Overington².

Azimuth (rad),	Elevation (rad)						
	0	$\pi/12$	$\pi/6$	$\pi/4$	$\pi/3$	$5\pi/12$	$\pi/2$
0	16 580	13 840	18 980	12 000	5 890	3 347	2 145
$\pi/4, 7\pi/4$	9 250	6 990	5 824	5 070	3 940	2 994	-
$\pi/2, 3\pi/2$	5 000	3 238	2 415	2 107	2 035	2 151	-
$3\pi/4, 5\pi/4$	4 385	2 597	1 658	1 357	1 364	1 597	-
π	4 728	2 665	1 569	1 213	1 179	1 466	-

The target signal flux, \mathfrak{I} , depends on the target brightness, measured in stellar magnitudes per resolution element, m_{RE} , where a resolution element is the solid angle subtense, Ω_{RE} , associated with a circle of angular diameter equal to $2.44 \lambda/D$.

$$\Omega_{\text{RE}} = \frac{1}{4} \pi (2.44 \lambda/D)^2 \quad (5)$$

A target with a circular cross-section of angular diameter θ_T subtends a solid angle of

$$\Omega_T = \frac{1}{4} \pi \theta_T^2 \quad (6)$$

Since a zero-magnitude star produces a flux density of³ 2.65×10^{-6} lumens/ m^2 then the total target signal flux will be

$$\mathfrak{I} = 2.65 \times 10^{-6} \times 10^{-(m_{\text{RE}}/2.5)} A (\Omega_T/\Omega_{\text{RE}}) \quad (7)$$

Assuming that the system spectral band may be considered to be centered at $\lambda = 0.55 \times 10^{-6} \text{ m}$, and taking note of the fact that the system's aperture diameter is $D = 1.6 \text{ m}$, we get from Eq. (5)

* Luminance brightness unit: $\text{cd}/\text{m}^2 \equiv \text{lumens}/\text{m}^2$ -steradian.

$$\Omega_{RE} = 5.525 \times 10^{-13} \text{ ster} \quad (8)$$

It is convenient to write

$$\begin{aligned} \Omega_T / \Omega_{RE} &= [\theta_T / (2.44 \lambda / D)]^2 \\ &= 33.4 (\theta_T / 4.85 \times 10^{-6})^2 \end{aligned} \quad (9)$$

Substituting Eq. (9) into Eq. (7) we get

$$\mathfrak{I} = 8.86 \times 10^{-6} \left(\frac{\theta_T}{4.85 \times 10^{-6}} \right)^2 10^{-(m_{RE}/2.5)_A} \quad (10)$$

When we substitute Eq. 's (2) and (10) into Eq. (1) we obtain for the ratio of the sky background flux to the target signal flux

$$\begin{aligned} \mathfrak{R} &= 0.547 B \theta \left(\frac{\theta_T}{4.85 \times 10^{-6}} \right)^{-2} 10^{(m_{RE}/2.5)} \\ &= 2.66 \times 10^{-6} B \left(\frac{\theta}{4.85 \times 10^{-6}} \right) \left(\frac{\theta_T}{4.85 \times 10^{-6}} \right)^{-2} 10^{(m_{RE}/2.5)}, \end{aligned} \quad (11)$$

which quantity we wish to evaluate for various target sizes and brightness, over the range of background brightness defined in Eq. (3). Sample results are listed in Table 2. As can be seen the value of \mathfrak{R} is greater than unity for all cases where the target brightness is as faint or fainter than m_{RE} equal 9^{th} magnitude per resolution element for the lower background sky brightness, i. e., $B = 1000 \text{ cd/m}^2$. For the higher sky brightness, i. e., $B = 6000 \text{ cd/m}^2$, the value of \mathfrak{R} is greater than unity for all cases where the target brightness is as faint or fainter than 7^{th} magnitude per resolution element.

TABLE 2a

Background To Target Ratio, \mathcal{R} , For Sky Brightness, B, Equal to 1000 lumens/m²-ster.

Values of \mathcal{R} are listed for target angular diameters, θ_T , from 2 arc seconds to 10 arc seconds and sensor field-of-view widths, θ , from θ_T to 10 arc seconds, for values of target brightness, $m_{\mathcal{R}}$, ranging from 4^m magnitude per resolution element to 12^m magnitude per resolution element.

$\theta / m_{\mathcal{R}}$	4	5	6	7	8	9	10	11	12
2.	5.29E-02	1.33E-01	3.34E-01	8.39E-01	2.11E+00	5.29E+00	1.53E+01	3.34E+01	8.39E+01
3.	7.94E-02	2.00E-01	5.01E-01	1.24E+00	3.16E+00	7.94E+00	2.00E+01	5.01E+01	1.24E+02
4.	1.04E-01	2.64E-01	6.68E-01	1.68E+00	4.22E+00	1.04E+01	2.64E+01	6.68E+01	1.68E+02
5.	1.32E-01	3.33E-01	8.35E-01	2.10E+00	5.27E+00	1.32E+01	3.33E+01	8.35E+01	2.10E+02
6.	1.59E-01	3.99E-01	1.00E+00	2.52E+00	6.32E+00	1.59E+01	3.99E+01	1.00E+02	2.52E+02
7.	1.85E-01	4.64E-01	1.17E+00	2.94E+00	7.38E+00	1.85E+01	4.64E+01	1.17E+02	2.94E+02
8.	2.12E-01	5.32E-01	1.34E+00	3.36E+00	8.43E+00	2.12E+01	5.32E+01	1.34E+02	3.36E+02
9.	2.38E-01	5.99E-01	1.50E+00	3.78E+00	9.49E+00	2.38E+01	5.99E+01	1.50E+02	3.78E+02
10.	2.65E-01	6.65E-01	1.67E+00	4.20E+00	1.05E+01	2.65E+01	6.65E+01	1.67E+02	4.20E+02
3.	3.53E-02	8.87E-02	2.23E-01	5.59E-01	1.41E+00	3.53E+00	8.87E+00	2.23E+01	5.59E+01
4.	4.71E-02	1.18E-01	2.97E-01	7.46E-01	1.87E+00	4.71E+00	1.18E+01	2.97E+01	7.46E+01
5.	5.88E-02	1.48E-01	3.71E-01	9.32E-01	2.34E+00	5.88E+00	1.48E+01	3.71E+01	9.32E+01
6.	7.04E-02	1.77E-01	4.45E-01	1.12E+00	2.81E+00	7.04E+00	1.77E+01	4.45E+01	1.12E+02
7.	8.24E-02	2.07E-01	5.20E-01	1.31E+00	3.28E+00	8.24E+00	2.07E+01	5.20E+01	1.31E+02
8.	9.41E-02	2.36E-01	5.94E-01	1.49E+00	3.75E+00	9.41E+00	2.36E+01	5.94E+01	1.49E+02
9.	1.06E-01	2.66E-01	6.68E-01	1.68E+00	4.22E+00	1.06E+01	2.66E+01	6.68E+01	1.68E+02
10.	1.18E-01	2.95E-01	7.42E-01	1.86E+00	4.68E+00	1.18E+01	2.95E+01	7.42E+01	1.86E+02
4.	2.65E-02	6.65E-02	1.67E-01	4.20E-01	1.05E+00	2.65E+00	6.65E+00	1.67E+01	4.20E+01
5.	3.31E-02	8.31E-02	2.09E-01	5.24E-01	1.32E+00	3.31E+00	8.31E+00	2.09E+01	5.24E+01
6.	3.97E-02	9.98E-02	2.51E-01	6.25E-01	1.58E+00	3.97E+00	9.98E+00	2.51E+01	6.25E+01
7.	4.68E-02	1.16E-01	2.92E-01	7.34E-01	1.84E+00	4.68E+00	1.16E+01	2.92E+01	7.34E+01
8.	5.29E-02	1.33E-01	3.34E-01	8.39E-01	2.11E+00	5.29E+00	1.33E+01	3.34E+01	8.39E+01
9.	5.94E-02	1.50E-01	3.74E-01	9.44E-01	2.37E+00	5.94E+00	1.50E+01	3.74E+01	9.44E+01
10.	6.62E-02	1.66E-01	4.18E-01	1.05E+00	2.63E+00	6.62E+00	1.66E+01	4.18E+01	1.05E+02
5.	2.12E-02	5.32E-02	1.34E-01	3.36E-01	8.43E-01	2.12E+00	5.32E+00	1.34E+01	3.36E+01
6.	2.57E-02	6.38E-02	1.60E-01	4.03E-01	1.01E+00	2.57E+00	6.38E+00	1.60E+01	4.03E+01
7.	2.97E-02	7.45E-02	1.87E-01	4.70E-01	1.18E+00	2.97E+00	7.45E+00	1.87E+01	4.70E+01
8.	3.39E-02	8.51E-02	2.14E-01	5.37E-01	1.35E+00	3.39E+00	8.51E+00	2.14E+01	5.37E+01
9.	3.81E-02	9.58E-02	2.41E-01	6.04E-01	1.52E+00	3.81E+00	9.58E+00	2.41E+01	6.04E+01
10.	4.24E-02	1.06E-01	2.67E-01	6.71E-01	1.69E+00	4.24E+00	1.06E+01	2.67E+01	6.71E+01
6.	1.74E-02	4.43E-02	1.11E-01	2.80E-01	7.03E-01	1.74E+00	4.43E+00	1.11E+01	2.80E+01
7.	2.06E-02	5.17E-02	1.30E-01	3.26E-01	8.20E-01	2.06E+00	5.17E+00	1.30E+01	3.26E+01
8.	2.35E-02	5.91E-02	1.48E-01	3.73E-01	9.33E-01	2.35E+00	5.91E+00	1.48E+01	3.73E+01
9.	2.65E-02	6.65E-02	1.67E-01	4.20E-01	1.05E+00	2.65E+00	6.65E+00	1.67E+01	4.20E+01
10.	2.94E-02	7.39E-02	1.84E-01	4.66E-01	1.17E+00	2.94E+00	7.39E+00	1.84E+01	4.66E+01
7.	1.51E-02	3.80E-02	9.55E-02	2.40E-01	6.02E-01	1.51E+00	3.80E+00	9.55E+00	2.40E+01
8.	1.73E-02	4.34E-02	1.07E-01	2.74E-01	6.88E-01	1.73E+00	4.34E+00	1.07E+01	2.74E+01
9.	1.95E-02	4.89E-02	1.23E-01	3.08E-01	7.74E-01	1.95E+00	4.89E+00	1.23E+01	3.08E+01
10.	2.16E-02	5.43E-02	1.36E-01	3.43E-01	8.60E-01	2.16E+00	5.43E+00	1.36E+01	3.43E+01
8.	1.32E-02	3.33E-02	8.35E-02	2.10E-01	5.27E-01	1.32E+00	3.33E+00	8.35E+00	2.10E+01
9.	1.49E-02	3.74E-02	9.40E-02	2.36E-01	5.99E-01	1.49E+00	3.74E+00	9.40E+00	2.36E+01
10.	1.65E-02	4.14E-02	1.04E-01	2.62E-01	6.59E-01	1.65E+00	4.14E+00	1.04E+01	2.62E+01
9.	1.19E-02	2.96E-02	7.42E-02	1.86E-01	4.68E-01	1.19E+00	2.96E+00	7.42E+00	1.86E+01
10.	1.31E-02	3.28E-02	8.23E-02	2.07E-01	5.20E-01	1.31E+00	3.28E+00	8.23E+00	2.07E+01
10.	1.06E-02	2.64E-02	6.68E-02	1.68E-01	4.22E-01	1.06E+00	2.64E+00	6.68E+00	1.68E+01

TABLE 2b

Background to Target Ratio, \mathfrak{R} , for Sky Brightness, B, Equal to 6000 lumens/m²-ster.

Values of \mathfrak{R} are listed for target angular diameters, θ_1 , from 2 arc seconds to 10 arc seconds and sensor field-of-view widths, θ , from θ_1 to 10 arc seconds, for values of target brightness, $m_{\mathfrak{R}}$, ranging from 4th magnitude per resolution element to 12th magnitude per resolution element.

θ	$m_{\mathfrak{R}}$	1	2	3	4	5	6	7	8	9	10	11	12
2.	3.18E-01	7.98E-01	7.98E-01	2.00E+00	5.04E+00	1.26E+01	3.18E+01	7.98E+01	1.90E+01	4.77E+01	1.20E+02	3.01E+02	5.04E+02
3.	4.77E-01	1.20E+00	3.01E+00	7.55E+00	1.90E+01	4.77E+01	1.20E+02	3.01E+02	7.55E+02	1.90E+03	4.77E+03	1.20E+04	3.01E+04
4.	6.35E-01	1.60E+00	4.01E+00	1.01E+01	2.53E+01	6.35E+01	1.60E+02	4.01E+02	1.01E+03	2.53E+03	6.35E+03	1.60E+04	4.01E+04
5.	7.94E-01	2.00E+00	5.01E+00	1.26E+01	3.16E+01	7.94E+01	2.00E+02	5.01E+02	1.26E+03	3.16E+03	7.94E+03	2.00E+04	5.01E+04
6.	9.53E-01	2.39E+00	6.01E+00	1.51E+01	3.79E+01	9.53E+01	2.39E+02	6.01E+02	1.51E+03	3.79E+03	9.53E+03	2.39E+04	6.01E+04
7.	1.11E+00	2.79E+00	7.02E+00	1.76E+01	4.45E+01	1.11E+02	2.79E+02	7.02E+02	1.76E+03	4.45E+03	1.11E+04	2.79E+04	7.02E+04
8.	1.27E+00	3.19E+00	8.02E+00	2.01E+01	5.06E+01	1.27E+02	3.19E+02	8.02E+02	2.01E+03	5.06E+03	1.27E+04	3.19E+04	8.02E+04
9.	1.43E+00	3.59E+00	9.02E+00	2.27E+01	5.59E+01	1.43E+02	3.59E+02	9.02E+02	2.27E+03	5.59E+03	1.43E+04	3.59E+04	9.02E+04
10.	1.59E+00	3.99E+00	1.00E+01	2.52E+01	6.35E+01	1.59E+02	3.99E+02	1.00E+03	2.52E+03	6.35E+03	1.59E+04	3.99E+04	1.00E+05
3.	2.12E-01	5.32E-01	1.34E+00	3.36E+00	8.43E+00	2.12E+01	5.32E+01	1.34E+02	3.36E+02	8.43E+02	2.12E+03	5.32E+03	1.34E+04
4.	2.82E-01	7.09E-01	1.78E+00	4.48E+00	1.12E+01	2.82E+01	7.09E+01	1.78E+02	4.48E+02	1.12E+03	2.82E+03	7.09E+03	1.78E+04
5.	3.53E-01	8.87E-01	2.23E+00	5.59E+00	1.41E+01	3.53E+01	8.87E+01	2.23E+02	5.59E+02	1.41E+03	3.53E+03	8.87E+03	2.23E+04
6.	4.24E-01	1.06E+00	2.67E+00	6.71E+00	1.69E+01	4.24E+01	1.06E+02	2.67E+02	6.71E+02	1.69E+03	4.24E+03	1.06E+04	2.67E+04
7.	4.94E-01	1.24E+00	3.12E+00	7.83E+00	1.97E+01	4.94E+01	1.24E+02	3.12E+02	7.83E+02	1.97E+03	4.94E+03	1.24E+04	3.12E+04
8.	5.65E-01	1.42E+00	3.56E+00	8.95E+00	2.26E+01	5.65E+01	1.42E+02	3.56E+02	8.95E+02	2.26E+03	5.65E+03	1.42E+04	3.56E+04
9.	6.35E-01	1.60E+00	4.01E+00	1.01E+01	2.53E+01	6.35E+01	1.60E+02	4.01E+02	1.01E+03	2.53E+03	6.35E+03	1.60E+04	4.01E+04
10.	7.06E-01	1.77E+00	4.45E+00	1.12E+01	2.82E+01	7.06E+01	1.77E+02	4.45E+02	1.12E+03	2.82E+03	7.06E+03	1.77E+04	4.45E+04
4.	1.59E-01	3.99E-01	1.00E+00	2.52E+00	6.35E+00	1.59E+01	3.99E+01	1.00E+02	2.52E+02	6.35E+02	1.59E+03	3.99E+03	1.00E+04
5.	1.99E-01	4.99E-01	1.25E+00	3.15E+00	7.90E+00	1.99E+01	4.99E+01	1.25E+02	3.15E+02	7.90E+02	1.99E+03	4.99E+03	1.25E+04
6.	2.38E-01	5.99E-01	1.50E+00	3.78E+00	9.49E+00	2.38E+01	5.99E+01	1.50E+02	3.78E+02	9.49E+02	2.38E+03	5.99E+03	1.50E+04
7.	2.78E-01	6.98E-01	1.75E+00	4.41E+00	1.11E+01	2.78E+01	6.98E+01	1.75E+02	4.41E+02	1.11E+03	2.78E+03	6.98E+03	1.75E+04
8.	3.18E-01	7.98E-01	2.00E+00	5.04E+00	1.26E+01	3.18E+01	7.98E+01	2.00E+02	5.04E+02	1.26E+03	3.18E+03	7.98E+03	2.00E+04
9.	3.57E-01	8.98E-01	2.26E+00	5.66E+00	1.42E+01	3.57E+01	8.98E+01	2.26E+02	5.66E+02	1.42E+03	3.57E+03	8.98E+03	2.26E+04
10.	3.97E-01	9.98E-01	2.51E+00	6.29E+00	1.58E+01	3.97E+01	9.98E+01	2.51E+02	6.29E+02	1.58E+03	3.97E+03	9.98E+03	2.51E+04
5.	1.27E-01	3.19E-01	8.02E-01	2.01E+00	5.06E+00	1.27E+01	3.19E+01	8.02E+01	2.01E+02	5.06E+02	1.27E+03	3.19E+03	8.02E+03
6.	1.52E-01	3.83E-01	9.62E-01	2.42E+00	6.07E+00	1.52E+01	3.83E+01	9.62E+01	2.42E+02	6.07E+02	1.52E+03	3.83E+03	9.62E+03
7.	1.78E-01	4.47E-01	1.12E+00	2.82E+00	7.08E+00	1.78E+01	4.47E+01	1.12E+02	2.82E+02	7.08E+02	1.78E+03	4.47E+03	1.12E+04
8.	2.03E-01	5.11E-01	1.28E+00	3.22E+00	8.09E+00	2.03E+01	5.11E+01	1.28E+02	3.22E+02	8.09E+02	2.03E+03	5.11E+03	1.28E+04
9.	2.29E-01	5.75E-01	1.44E+00	3.63E+00	9.11E+00	2.29E+01	5.75E+01	1.44E+02	3.63E+02	9.11E+02	2.29E+03	5.75E+03	1.44E+04
10.	2.54E-01	6.38E-01	1.60E+00	4.03E+00	1.01E+01	2.54E+01	6.38E+01	1.60E+02	4.03E+02	1.01E+03	2.54E+03	6.38E+03	1.60E+04
6.	1.03E-01	2.66E-01	6.68E-01	1.68E+00	4.22E+00	1.03E+01	2.66E+01	6.68E+01	1.68E+02	4.22E+02	1.03E+03	2.66E+03	6.68E+03
7.	1.24E-01	3.10E-01	7.80E-01	1.96E+00	4.92E+00	1.24E+01	3.10E+01	7.80E+01	1.96E+02	4.92E+02	1.24E+03	3.10E+03	7.80E+03
8.	1.41E-01	3.55E-01	8.91E-01	2.24E+00	5.62E+00	1.41E+01	3.55E+01	8.91E+01	2.24E+02	5.62E+02	1.41E+03	3.55E+03	8.91E+03
9.	1.59E-01	3.99E-01	1.00E+00	2.52E+00	6.35E+00	1.59E+01	3.99E+01	1.00E+02	2.52E+02	6.35E+02	1.59E+03	3.99E+03	1.00E+04
10.	1.76E-01	4.43E-01	1.11E+00	2.80E+00	7.05E+00	1.76E+01	4.43E+01	1.11E+02	2.80E+02	7.05E+02	1.76E+03	4.43E+03	1.11E+04
7.	9.08E-02	2.28E-01	5.73E-01	1.44E+00	3.61E+00	9.08E+00	2.28E+01	5.73E+01	1.44E+02	3.61E+02	9.08E+02	2.28E+03	5.73E+03
8.	1.04E-01	2.61E-01	6.55E-01	1.64E+00	4.13E+00	1.04E+01	2.61E+01	6.55E+01	1.64E+02	4.13E+02	1.04E+03	2.61E+03	6.55E+03
9.	1.17E-01	2.93E-01	7.36E-01	1.85E+00	4.65E+00	1.17E+01	2.93E+01	7.36E+01	1.85E+02	4.65E+02	1.17E+03	2.93E+03	7.36E+03
10.	1.30E-01	3.26E-01	8.18E-01	2.06E+00	5.16E+00	1.30E+01	3.26E+01	8.18E+01	2.06E+02	5.16E+02	1.30E+03	3.26E+03	8.18E+03
8.	7.94E-02	2.00E-01	5.01E-01	1.26E+00	3.16E+00	7.94E+00	2.00E+01	5.01E+01	1.26E+02	3.16E+02	7.94E+02	2.00E+03	5.01E+03
9.	8.94E-02	2.24E-01	5.64E-01	1.42E+00	3.56E+00	8.94E+00	2.24E+01	5.64E+01	1.42E+02	3.56E+02	8.94E+02	2.24E+03	5.64E+03
10.	9.93E-02	2.49E-01	6.26E-01	1.57E+00	3.95E+00	9.93E+00	2.49E+01	6.26E+01	1.57E+02	3.95E+02	9.93E+02	2.49E+03	6.26E+03
9.	7.06E-02	1.77E-01	4.45E-01	1.12E+00	2.81E+00	7.06E+00	1.77E+01	4.45E+01	1.12E+02	2.81E+02	7.06E+02	1.77E+03	4.45E+03
10.	7.84E-02	1.97E-01	4.95E-01	1.24E+00	3.12E+00	7.84E+00	1.97E+01	4.95E+01	1.24E+02	3.12E+02	7.84E+02	1.97E+03	4.95E+03
10.	6.35E-02	1.60E-01	4.01E-01	1.01E+00	2.53E+00	6.35E+00	1.60E+01	4.01E+01	1.01E+02	2.53E+02	6.35E+02	1.60E+03	4.01E+03

In general we may say that a value of \mathcal{R} as great as unity significantly degrades system performance relative to what it might be in the absence of the daytime sky background—and that larger values result in larger degradations. In the next section we will develop quantitative estimates of the extent of the degradation.

1.3 System Performance Degradation

If the wavefront sensor of the compensated imaging system is perfectly aligned, which we shall assume to be the case, then the only fundamental problem produced by the presence of the daytime sky background is the introduction of additional shot noise in the detector output. It is easy to see that with a ratio of background flux to target flux of \mathfrak{R} , the rms noise level from the detector will be increased by a factor of $(\mathfrak{R} + 1)^{1/2}$, and the achievable signal-to-noise ratio will be reduced by a factor of $(\mathfrak{R} + 1)^{-1/2}$. To take proper account of the effect of background on system performance it is (at least nominally) necessary to recall that in practice the compensated imaging system's operation is adjusted to achieve, to the extent possible, a balance between wavefront fitting error, time lag induced error, and shot noise induced error. These last two errors are both dependent on the servo bandwidth, which is adjustable. As the servo bandwidth is increased the time lag error is reduced, but the shot-noise error is increased, and vice versa. Nominally the servo bandwidth is chosen based on the target brightness, measured in stellar magnitudes per resolution element, as it is this together with bandwidth that determines the achieved signal-to-noise ratio. Extensive calculations of the trade-off's involved have been performed by Itek, to provide curves of achievable performance as a function of target brightness for various engagement conditions (i. e., for various atmospheric turbulence distributions and target angular velocities).⁴ It is obvious from consideration of data such as this that the dependence of system performance on target brightness (for night sky background) is quite complex.

Fortunately, to take full account of the effect of daylight sky brightness on system performance it is not actually necessary to repeat all of the trade-off optimization work with each combination of background and target fluxes. Instead, we can make use of the existing results for nighttime

operation by defining the concept of an equivalent target brightness. For each combination of background and target fluxes there is some constant which relates the measurement/servo bandwidth to a shot-noise limited signal-to-noise ratio or rather to the shot-noise limited rms wavefront measurement error. This same constant also applies to the night sky case for some particular target brightness. This is the equivalent target brightness. We may equate the combination of actual target brightness, m_{RE} , target size, θ_T , field-of-view width, θ , and sky background brightness, B , with this equivalent brightness, \tilde{m}_{RE} . We can then look up the system performance for the equivalent target brightness under nighttime sky background conditions, and apply what we find to the corresponding daytime sky background situation.

Considering that the shot-noise limited performance in the presence of sky background is degraded by a factor of $(\mathfrak{R} + 1)^{-1/2}$, and since the shot-noise limited performance against a nighttime sky varies, as a function of target brightness, as $10^{-(m_{RE}/5)}$, then it follows that the equivalent brightness, \tilde{m}_{RE} , is related to the actual target brightness, m_{RE} , by the equation

$$10^{-(\tilde{m}_{RE}/5)} = (\mathfrak{R} + 1)^{-1/2} 10^{-(m_{RE}/5)} \quad (12)$$

Solving for the equivalent brightness, we get

$$\tilde{m}_{RE} = m_{RE} + 2.5 \log_{10} (\mathfrak{R} + 1) \quad (13)$$

In Table 3 we show the values of the equivalent target brightness for the same set of conditions of actual target brightness, target size, field-of-view widths and sky brightness as were treated in Table 2. Accordingly, as we take the useful night sky performance cut-off to occur at 10TH, 12TH, or 14TH magnitude per resolution element, the daytime sky cut-off can be seen to occur at smaller but often still interesting levels of actual target brightness.

TABLE 3a

Equivalent Target Brightness, \tilde{m}_{TE} , for Sky Brightness, B, Equal to 1000 lumens/m²-ster.

Values of \tilde{m}_{TE} (in units of stellar magnitude per resolution element) are listed for target angular diameters, θ_T , from 2 arc seconds to 10 arc seconds and sensor field-of-view widths, θ , from θ_T to 10 arc seconds, for values of the actual target brightness, m_{TE} , ranging from 4^m magnitude per resolution element to 12^m magnitude per resolution element.

$\theta \backslash m_{\text{TE}}$	4	5	6	7	8	9	10	11	12
3.	4.1	5.1	6.3	7.7	9.2	11.0	12.9	14.8	16.7
4.	4.1	5.2	6.4	7.9	9.5	11.4	13.3	15.3	17.3
5.	4.1	5.3	6.6	8.1	9.8	11.7	13.7	15.8	17.8
6.	4.2	5.4	6.7	8.2	10.0	11.9	13.8	15.8	18.0
7.	4.2	5.4	6.8	8.5	10.3	12.2	14.2	16.2	18.2
8.	4.2	5.5	6.9	8.6	10.4	12.4	14.3	16.3	18.3
9.	4.2	5.5	7.0	8.7	10.6	12.5	14.5	16.4	18.4
10.	4.3	5.6	7.1	8.8	10.7	12.6	14.6	16.6	18.6
3.	4.7	5.1	6.2	7.5	9.0	10.6	12.5	14.4	16.4
4.	4.0	5.1	6.3	7.6	9.1	10.9	12.8	14.7	16.7
5.	4.1	5.1	6.3	7.7	9.3	11.1	13.0	15.0	16.9
6.	4.1	5.2	6.4	7.8	9.5	11.3	13.2	15.1	17.1
7.	4.1	5.2	6.5	7.9	9.6	11.4	13.3	15.3	17.3
8.	4.1	5.2	6.5	8.0	9.7	11.5	13.5	15.5	17.4
9.	4.1	5.3	6.6	8.1	9.8	11.7	13.6	15.6	17.6
10.	4.1	5.3	6.6	8.1	9.9	11.8	13.7	15.7	17.7
4.	4.0	5.1	6.2	7.4	8.8	10.4	12.2	14.1	16.1
5.	4.0	5.1	6.2	7.5	8.9	10.6	12.4	14.4	16.3
6.	4.0	5.1	6.2	7.5	9.0	10.7	12.6	14.5	16.5
7.	4.0	5.1	6.3	7.6	9.1	10.9	12.8	14.7	16.7
8.	4.1	5.1	6.3	7.7	9.2	11.0	12.9	14.8	16.8
9.	4.1	5.2	6.3	7.7	9.3	11.1	13.0	15.0	16.9
10.	4.1	5.2	6.4	7.8	9.4	11.2	13.1	15.1	17.1
5.	4.0	5.1	6.1	7.3	8.7	10.2	12.0	13.9	15.8
6.	4.0	5.1	6.2	7.4	8.8	10.4	12.2	14.1	16.0
7.	4.0	5.1	6.2	7.4	8.8	10.5	12.3	14.2	16.2
8.	4.0	5.1	6.2	7.5	8.9	10.6	12.4	14.4	16.3
9.	4.0	5.1	6.2	7.5	9.0	10.7	12.6	14.5	16.5
10.	4.0	5.1	6.3	7.6	9.1	10.8	12.7	14.6	16.6
6.	4.0	5.0	6.1	7.3	8.6	10.1	11.8	13.7	15.7
7.	4.0	5.1	6.1	7.3	8.7	10.2	12.0	13.9	15.8
8.	4.0	5.1	6.2	7.3	8.7	10.3	12.1	14.0	16.0
9.	4.0	5.1	6.2	7.4	8.8	10.4	12.2	14.1	16.1
10.	4.0	5.1	6.2	7.4	8.8	10.5	12.3	14.2	16.2
7.	4.0	5.0	6.1	7.2	8.5	10.0	11.7	13.6	15.5
8.	4.0	5.0	6.1	7.3	8.6	10.1	11.8	13.7	15.6
9.	4.0	5.1	6.1	7.3	8.6	10.2	11.9	13.8	15.8
10.	4.0	5.1	6.1	7.3	8.7	10.2	12.0	13.9	15.9
8.	4.0	5.0	6.1	7.2	8.5	9.9	11.6	13.4	15.4
9.	4.0	5.0	6.1	7.2	8.5	10.0	11.7	13.5	15.5
10.	4.0	5.0	6.1	7.3	8.5	10.1	11.8	13.6	15.6
9.	4.0	5.0	6.1	7.2	8.4	9.8	11.5	13.3	15.2
10.	4.0	5.0	6.1	7.2	8.5	9.9	11.6	13.4	15.3
10.	4.0	5.0	6.1	7.2	8.4	9.8	11.4	13.2	15.1

TABLE 3b

Equivalent Target Brightness, \bar{m}_{θ_1} , for Sky Brightness, B, Equal to 6000 lumens/m²-ster.

Values of \bar{m}_{θ_1} (in units of stellar magnitude per resolution element) are listed for target angular diameters, θ_1 , from 2 arc seconds to 10 arc seconds and sensor field-of-view widths, θ , from θ_1 to 10 arc seconds, for values of the actual target brightness, m_{θ_1} , ranging from 4^H magnitude per resolution element to 12^H magnitude per resolution element.

$\theta_1 = 2$	θ	m_{θ_1}	4	5	6	7	8	9	10	11	12
3.	3.	4.3	4.3	5.6	7.2	9.0	10.8	13.0	14.8	16.8	18.8
	4.	4.4	5.9	7.7	9.6	11.3	13.2	15.2	17.2	19.2	21.2
	5.	4.5	6.0	7.9	9.8	11.8	13.8	15.8	17.8	19.8	21.8
	6.	4.6	6.2	8.1	10.0	12.0	14.0	16.0	18.0	19.9	20.1
	7.	4.7	6.3	8.3	10.2	12.1	14.1	16.1	18.1	20.1	20.3
	8.	4.8	6.4	8.4	10.3	12.2	14.2	16.2	18.2	20.3	20.4
	9.	4.9	6.5	8.5	10.4	12.3	14.3	16.3	18.3	20.4	20.5
	10.	5.0	6.7	8.5	10.4	12.4	14.4	16.4	18.4	20.4	20.5
3.	3.	4.2	5.5	6.9	8.6	10.4	12.4	14.3	16.3	18.3	20.3
	4.	4.3	5.6	7.1	8.8	10.7	12.7	14.6	16.6	18.6	20.6
	5.	4.3	5.7	7.3	9.0	10.9	12.9	14.9	16.9	18.9	20.9
	6.	4.4	5.8	7.4	9.2	11.1	13.1	15.1	17.1	19.1	21.1
	7.	4.4	5.9	7.5	9.4	11.3	13.3	15.3	17.2	19.2	21.2
	8.	4.5	6.0	7.6	9.5	11.4	13.4	15.4	17.4	19.4	21.4
	9.	4.5	6.0	7.7	9.6	11.5	13.5	15.5	17.5	19.5	21.5
	10.	4.6	6.1	7.8	9.7	11.7	13.6	15.6	17.6	19.6	21.6
4.	4.	4.2	5.4	6.8	8.4	10.2	12.1	14.0	16.0	18.0	20.0
	5.	4.2	5.4	6.9	8.5	10.4	12.3	14.3	16.3	18.2	20.2
	6.	4.2	5.5	7.0	8.7	10.6	12.5	14.5	16.4	18.4	20.4
	7.	4.3	5.6	7.1	8.8	10.7	12.6	14.6	16.6	18.6	20.6
	8.	4.3	5.6	7.2	9.0	10.8	12.8	14.8	16.8	18.8	20.8
	9.	4.3	5.7	7.3	9.1	11.0	12.9	14.9	16.9	18.9	20.9
	10.	4.4	5.8	7.4	9.2	11.1	13.0	15.0	17.0	19.0	21.0
5.	5.	4.1	5.3	6.6	8.2	10.0	11.8	13.8	15.8	17.8	19.8
	6.	4.2	5.4	6.7	8.3	10.1	12.0	14.0	16.0	18.0	20.0
	7.	4.2	5.4	6.8	8.5	10.3	12.2	14.1	16.1	18.1	20.1
	8.	4.2	5.4	6.9	8.6	10.4	12.3	14.3	16.3	18.3	20.3
	9.	4.2	5.5	7.0	8.7	10.5	12.4	14.4	16.4	18.4	20.4
	10.	4.2	5.5	7.0	8.8	10.6	12.5	14.5	16.5	18.5	20.5
6.	6.	4.1	5.3	6.6	8.1	9.8	11.7	13.6	15.6	17.6	19.6
	7.	4.1	5.3	6.6	8.2	9.9	11.8	13.8	15.7	17.7	19.7
	8.	4.1	5.3	6.7	8.3	10.1	11.9	13.9	15.9	17.9	19.9
	9.	4.2	5.4	6.8	8.4	10.2	12.1	14.0	16.0	18.0	20.0
	10.	4.2	5.4	6.8	8.4	10.3	12.2	14.1	16.1	18.1	20.1
7.	7.	4.1	5.2	6.5	8.0	9.7	11.5	13.4	15.4	17.4	19.4
	8.	4.1	5.3	6.5	8.1	9.8	11.6	13.5	15.5	17.5	19.5
	9.	4.1	5.3	6.6	8.1	9.9	11.7	13.6	15.6	17.6	19.6
	10.	4.1	5.3	6.6	8.2	10.0	11.8	13.8	15.8	17.8	19.8
8.	8.	4.1	5.2	6.4	7.9	9.5	11.4	13.3	15.3	17.3	19.3
	9.	4.1	5.2	6.5	8.0	9.6	11.5	13.4	15.4	17.4	19.4
	10.	4.1	5.2	6.5	8.0	9.7	11.6	13.5	15.5	17.5	19.5
9.	9.	4.1	5.2	6.4	7.8	9.5	11.3	13.2	15.1	17.1	19.1
	10.	4.1	5.2	6.4	7.9	9.5	11.4	13.3	15.3	17.3	19.3
10.	10.	4.1	5.2	6.4	7.8	9.4	11.2	13.1	15.0	17.0	19.0

1.4 References for Chapter I

1. K. Ya. Kondratyev, Radiation In The Atmosphere, (Academic Press, 1969, New York).
2. Ian Overington, Vision And Acquisition, (Crane, Russak and Co., 1976, New York)
3. C. W. Allen, Astrophysical Quantities, (Athlone Press, 1955, London).
4. This reiference will be made available to qualified military and government agencies on request from RADC (OCSE) Griffiss AFB NY 13441.

Chapter II

Configuration and Analysis

for an

UpLink Experiment/Demonstration

2.1 Introduction to Chapter II

Evaluation and demonstration of the technology associated with an UpLink adaptive optics transmitter is a critical requirement of the SLC program as well as of several other programs of potential interest to various user communities. In this chapter we shall be interested in the definition and evaluation of an experimental program that will allow this assessment and demonstration to be accomplished—and which will, of course, force the necessary degree of advancement of the technology. The ultimate objective of the program will be to obtain assurance that we know how to build an UpLink adaptive optics transmitter, capable of nearly diffraction limited performance. In defining the program we have taken the following positions. 1) That the experiment design should be such as to minimize the cost for experimental aspects that are not part of the adaptive optics transmitter per se. 2) That the adaptive optics transmitter must be large enough to not only challenge the device fabrication technology, but also to provide a significant improvement in antenna gain relative to what could be achieved without adaptive optics. However, it need not be as large as the transmitter that would be used with an operational UpLink system. 3) That an experimental program consisting of several parts, each designed to explore different aspects of the UpLink adaptive optics technology would be acceptable if (a) taken together the sum of the experiments provide coverage of all of the technical questions, and if (b) the division of the program into several parts provides a logical and cost effective approach.

In the next section we shall offer some specific comments concerning the driving aspects of the design of the experiment(s), and will try to develop some general guidance for the design. The section after that will present a suggested experiment package. This will be followed by sections analyzing various performance considerations for the experiment(s).

2.2 General Considerations

The key to an evaluation of the performance of an UpLink adaptive optics transmitter is a measurement of the transmitter antenna gain. The SLC system will have a very large diameter relay mirror in a synchronous orbit position which will reflect the incident laser energy back toward the earth. Assuming, that the relay mirror has associated with it a suitably positioned and sufficiently intense beacon, then a well designed adaptive optics UpLink laser transmitter should be able to achieve nearly diffraction limited performance in delivering power to the relay mirror. We would like to carry out an experiment using a full size UpLink transmitter and a suitably sized relay mirror, which would demonstrate the ability of the UpLink transmitter to do this by monitoring the laser energy returned to the ground via the relay mirror. Not only would such a system allow full validation of the technology involved, but with only a "modest" power laser source it could provide a reduced but none-the-less useful level of channel capacity for SLC.

Unfortunately this type of experiment is more complex and more expensive than we should consider undertaking in a near term, initial evaluation/demonstration of UpLink adaptive optics laser transmitter technology. Fortunately, it is not necessary to go to anything like this level of system verisimilitude to evaluate/demonstrate the UpLink transmitter technology. First of all it is not necessary to have a large diameter relay mirror satellite in orbit. All we want to do is confirm that the antenna gain of the UpLink adaptive optics laser transmitter is as large as expected—and to do this it is sufficient that we have some small diameter unit which will allow us to determine the power density at the orbital position. Strictly speaking, it is not even necessary that this sensor be located in a synchronous orbit, or even at a similar range.

Moreover, it is not required that all aspects of the propagation problem be exercised in one experiment. What is necessary is that in some form each aspect of the problem be exercised during a set of experiments and

that we be able to compare experimental results with theory. This will allow us to develop the conclusion that we understand all relevant aspects of the problem and that as far as the UpLink portion of the SLC concept is concerned we need not worry about any surprises at a fundamental (propagation phenomenology) level. If, in addition the experimental adaptive optics laser transmitter has a reasonably large aperture i. e. , D/r_0 is large enough, say ten or greater, so that the adaptive optics hardware represents a nontrivial correction capability, then we could conclude from a successful set of experiments that we are "on top" of the situation.

The possibility of factoring the experimental problem into a set of distinct tests offers us some very useful options. We are particularly concerned with the cost/complexity associated with the isoplanatism problem and the corresponding difficulty of station-keeping to maintain the proper distance between the beacon satellite and the satellite that will fly in the position of the relay mirror, (which latter satellite will provide the basis for measurement of the UpLink laser transmitter's antenna gain.) In fact, we feel that the station-keeping requirement gets us into a set of cost constraints that must be avoided. We shall outline in the next section an experimental concept with no distinct beacon satellite— this experiment being based on a single very simple (low cost?) satellite. This means that we will not only have an isoplanatism problem, but that we will not be able to vary the station-keeping error so that we can see how the anisoplanatism effect varies with station-keeping error. But the satellite should be low cost.

To augment this experiment and allow all aspects of the propagation problem to be exercised we would also run an experiment utilizing an aircraft in place of the satellite at the far end of the UpLink beam. The aircraft experiment will not involve us with the problem of sending a collimated beam all the way up through the atmosphere—but we will get a handle on that part of the propagation phenomenology in the satellite experiment. What we will get from the aircraft experiment that we cannot afford to try to get from the satellite experiment will be the ability to change the angular

separation between the beacon and the real aim-point of the UpLink transmitter, and the ability to work at various zenith angles and ranges. From the first experiment we will get data that will allow us to confirm that we do understand how anisoplanatism will effect the antenna gain of the UpLink transmitter. From the second we will get the ability to experimentally verify our theoretical understanding of how servo bandwidth and the size of r_0 effects the antenna gain of the UpLink transmitter. Also, we will be able to determine from this the validity of our understanding of beacon intensity scintillation on antenna gain.

In general our philosophy in configuring both a satellite experiment and an aircraft experiment is that the aircraft experiment will be versatile and allow us to test all aspects of the theory that are of interest to us. The satellite experiment on the other hand will not be particularly versatile. It will be constrained by cost considerations, and will have as virtually its only objectives the need to provide assurance that sending a collimated beam all the way through the upper atmosphere, (which the aircraft experiment does not probe), and then into deep space does not introduce any great surprises. The satellite experiment will also, of course, provide a kind of "cap stone", demonstration that the UpLink adaptive optics laser transmitter can indeed transmit to a relay mirror satellite in deep space with the theoretically expected antenna gain.

The section after this will take up the description of the aircraft and satellite experiments. Analytical considerations for experiment design are presented in the section after that.

2.3 Experiment Description

It will be convenient to first describe the aircraft experiment and then turn our attention to the task of describing the satellite version of the UpLink experiment. This will allow us to apply our attention to a rather straight forward experiment first, and only later take up a consideration of the "machination" we have to go through to have a suitable beacon with a low cost spacecraft. In the following two subsections we discuss first the aircraft experiment and then the satellite experiment.

2.3.1 Aircraft Experiment

For the aircraft experiment we would utilize the Compensated Imaging System adaptive optics installed in the 1.6 m diameter telescope at the DARPA AMOS facility, as the laser beam transmitter. An aircraft mounted beacon and laser power detector would be used to provide a reference source for the adaptive optics and to evaluate the effective antenna gain of the laser transmitter. The aircraft would fly at some constant altitude in a circular path, centered about the AMOS facility. Depending on the choice of aircraft, the flight altitude could be anywhere from say 2.5 km up to 10 km, or possibly up to 15 km, or even 20 km. The radius of the circular path will be somewhere between 5.0 km and 30 km depending on the desired propagation effects, and the aircraft velocity will, at least nominally, be $V=200$ m/sec.

A pod, under two meters in length will be carried by the aircraft. It would be mounted so that the length of the pod can be viewed from the AMOS facility as the aircraft flies its' circular pattern. A relatively low power discharge lamp, mounted near the front end of the pod will radiate isotropically (or at least hemispherically). For a suitable choice of lamp, the lamp will appear as a point source, i. e., unresolved at the telescopes diffraction limit at all ranges of interest, and will be brighter than a zero-magnitude star even at the maximum range of interest. Nominally we consider a high pressure mercury lamp which, with a 200 W input can provide 1000 lumens/ster, virtually isotropic, from a source area of about 2.2 mm x 0.6 mm. This means that the discharge lamp will provide a more than adequate beacon for use by the laser transmitter's adaptive optics wavefront distortion sensor. We shall examine this in more detail later—for the moment it is sufficient to note that the Compensated Imaging Systems' adaptive optics can work quite well with an unresolved target whose brightness is 6th magnitude. In fact, we may have to attenuate such a bright beacon to keep it from saturating the adaptive optics sensor.

Also mounted on the pod will be a single detector about 1mm x 1 mm in size, with a moderately narrow band optical filter. Except for the optical filter the detector will have no optics. The field-of-view of both the beacon and the detector will be large since neither will have optics and thus, will be able to radiate into/collect radiation from any direction within a hemisphere. The large field-of-view of both the beacon and the detector insure that no special stabilization of the pod is required. The detector will be mounted on a track with an electrically controlled drive arrangement so that its distance behind the beacon can be remotely controlled. Varying this distance will result in a variation in the anisoplanatism effort.

In addition to the beacon and the detector, the pod will have an rf transmitter which will provide a data link to the AMOS facility. The intensity of the signal developed by the detector will be reported to the facility, where it can be used for pointing control purposes and also will be recorded for the subsequent data analysis. This data link will periodically report the position of the detector but most of the time will be reporting the intensity of the transmitted laser beam falling on the detector. The transmitted laser beam will be sent as a chopped signal (to facilitate distinguishing the laser signal from the background flux), and electronics within the pod will demodulate the chopped signal and develop an estimate of the intensity of the laser signal. It is that intensity estimate that will be transmitted.

In operation, the aircraft would fly a circular path at the desired altitude and range, oriented so that the pod can be seen from the AMOS facility. The beacon will be turned on and should be clearly visible at the observatory. * The 1.6 m telescope will be pointed toward the aircraft and be driven to nominally track the aircraft. Once the adaptive optics system has detected the beacon and locked on to it, the shearing interferometer signals would be used to drive the telescope so that it

* The brightness of the beacon should be great enough that daytime as well as nighttime operation will be possible.

(in conjunction with the fast steering mirror) precisely tracks the beacon. The adaptive optics control electronics will be modified so as to allow operation in any of the following three modes: 1) normal adaptive optics control, 2) operation with the deformable mirror drive disabled, and 3) operation with the deformable mirror drive disabled and the fast steering mirror drive operating at a reduced bandwidth.

To boresight the system, i. e. , to get the transmitted laser beam "lined-up" with the wavefront sensor, a pointing bias control voltage will be added to the fast steering mirror signal. This bias control will be varied so as to scan the transmitted beam over the area on the pod in the vicinity of the beacon. By monitoring the telemetry signal from the pod, it will be possible to adjust the bias so as to center the laser beam on the detector. The servo bandwidth for this centering process will deliberately be kept low enough that it only compensates for the boresight error and does not correct for the zero-mean high speed pointing errors induced by atmospheric turbulence.

With the laser transmitter operating, with the beacon being tracked, and with the boresight error compensated, measurements will be made of the average laser power density on the detector for each of the three modes of operation of the adaptive optics control. The laser transmitter will in addition have the ability, by inserting special optics directly in front of the laser, to underfill the telescope aperture so that only a 0.03 m diameter circular region is illuminated, with all of the laser power passing through this small region. Measurements of laser power density on the detector will also be made with this underfilled aperture. Based on these measurements the laser transmitter antenna gain will be calculated for each of the three conditions of no adaptive optics, fast tracking correction only, and full adaptive optics. (The antenna gain results will have a meaningful absolute value based on the fact that for the underfilled aperture the antenna gain will have very nearly its diffraction limited value, as r_0 will be significantly larger

than 0.03 m.) By varying the pointing bias in a slow scan raster pattern it will be possible to evaluate not only the absolute antenna gain but also the average antenna gain side lobe pattern.

Experiments will be run with the following variations:

- 1) Aircraft range and altitude,
- 2) Time of day,
- 3) Distance on the pod between the beacon and the detector,
- 4) Adaptive optics servo bandwidth.

In Fig's 3-6 we show the implications of various choices at aircraft range and altitude for several propagation related parameters. By suitable choice of range and altitude the aircraft experiment will be able to explore the implications of various combinations of these parameter values. The time of day variations will let us examine how turbulence strength varies with time. The variation of the separation between the beacon and the detector will provide us with a direct assessment of the effect of anisoplanatism, while the variability of the servo bandwidth will allow an evaluation of the dependence on that quantity of the antenna gain.

The key thing about the aircraft experiments is that it will allow an extensive set of tests of theory against experiment, providing assurance that we do indeed understand the things that affect the performance of an adaptive optics system. But equally important is the fact that it will allow a demonstration that a large aperture adaptive optics laser transmitter can achieve a nearly diffraction limited antenna gain when operating over a substantial atmospheric path. What it will leave undone is to establish the fact that there are not surprises lurking in the problem of sending a nearly collimated laser beam through the upper atmosphere. This one matter will be addressed in the satellite experiment discussed in the next section.

Before leaving the subject of the aircraft experiment it is worth devoting some space to a consideration of the implementation and schedule

aspects of this experiment. We assume that the adaptive optics system that is now being prepared for installation in the 1.6 m diameter AMOS telescope as part of the Compensated Imaging System will be available for this aircraft target/laser transmitter experiment, as well as the 1.6 m diameter AMOS telescope itself. The adaptive optics system would require only the very minor modification of replacing * the camera with a lower power visible laser source—about one milliwatt at 5000 Å or 6000 Å, with intensity modulation (chopping) at several kilohertz. The laser source would require some special (though quite simple) optics to couple it into the optical train of the adaptive optics system. These special optics would have to have the ability to fill the full 1.6 m diameter telescope aperture with the laser beam, and on command, by a change of element position, fill only a 0.03 m diameter portion of the telescope aperture. The design, assembly, and installation of the laser and its special optics onto the Compensated Imaging System is a small effort which should be accomplishable within six months.

In conjunction with the installation of the laser it will be necessary to modify the Compensated Imaging System so as to prevent scattered light from the laser from "blinding" the wavefront distortion sensor. This can be accomplished by installing narrow band blocking filters in the portion of the optical path used only for the wavefront sensor, i. e., the portion between the presently installed beamsplitter and the photo multipliers. This too should represent a rather minor hardware modification, with a rather short time required for its accomplishment.

Probably the largest change that will have to be made to the Compensated Imaging System to turn it into an adaptive optics laser transmitter for the aircraft experiment is modification of the system software. It is

* With a dichroic beamsplitter, it should not even be necessary to remove the camera. The laser could possibly be installed along side the camera and through the dichroic beamsplitter share with the camera the optical path through the adaptive optics train.

difficult to scope the size of that effort without a much more detailed examination of the problem than we are prepared to carry out here. None-the-less, we feel fairly confident that the necessary software development, installation, and debugging can be accomplished in less than 18 months. It therefore, appears to us to be the case that the Compensated Imaging System once operating in the mode it was originally designed for, could be converted into an adaptive optics laser transmitter for the aircraft experiment within a year and a half of the time from when such a conversion effort was started.

The design and fabrication of the beacon/detector pod to go on the aircraft poses virtually no electro-optical challenges. There are no critical alignments, the beacon power will be modest (commercial sources at the required brightness and flux level are common), and the required detector sensitivity is negligible. The principal difficulties will be those associated with assuring aircraft safety and atmospheric pressure.† Accordingly, it would appear that pod could be designed, built, installed on the aircraft and checked out within 12 to 18 months of the start of an effort to accomplish this.*

Based on the above listed considerations we believe that the aircraft experiment could be producing useful data within two years. This two year schedule allows six months for preliminary data taking, analysis, and such revision of the test plans as may be found necessary. Key to this is, of

* We have not examined what is involved but assume that there will be no difficulty in establishing the required rf data line between the aircraft (pod) and the AMOS facility.

† From consideration of the data in Fig's 3-6 there does not appear to be any special reason to require operation of the aircraft above 10 km (30,000 ft.). Accordingly the aircraft used for this experiment need not be particularly exotic.

course, the availability of the Compensated Imaging System, installed and operational on the AMOS 1.6 m diameter telescope — and of course, the availability of the AMOS 1.6 m telescope facility, and of a suitable aircraft.

2.3.2 Satellite Experiment

The objective of the satellite experiment is to provide assurance that nothing unexpected happens when we send a collimated beam through the upper atmosphere. All other aspects of the adaptive optics laser transmitter performance will have been explored in the aircraft experiment and diffraction limited transmitter performance demonstrated there, for the satellite experiment we have only one thing to test. We wish to do that as expeditiously and cost-effectively as possible. We do not wish to run a simulation/demonstration and will accept simplifications so long as they allow the basic test data to be obtained. We will do this even though the simplifications are features that accentuate the fact that this is not a simulation of an SLC system, but just a test of one aspect of the UpLink portion of an SLC system!

The basic problem we are concerned with in defining the satellite experiment is the cost, complexity, and development schedule for the satellite per se. We don't want to have to invest in a major satellite development effort just to test the ground based laser transmitter. There are two things that tend to make the satellite very expensive. These are 1) the fine pointing required of the beacon (which of course, means amongst other things that the satellite must be very well stabilized in orientation, and 2) the need to maintain a well defined separation between the beacon satellite unit and the laser receiver satellite unit. (At synchronous altitude this separation is of the order of 800 m.) The cost for a satellite system like this would be several ten's of millions of dollars, which is entirely out of line with the objectives of the satellite experiment. We shall define a much simpler satellite which should cost orders of magnitude less, and which will be only just sufficient to allow the basic objectives of the satellite experiment to be achieved.

We first of all abandon the concept of separate locations for the beacon and the laser detector. The station keeping requirements to keep two space

craft properly separated* leads to high cost. If we back away from that requirement and accept collocation of the beacon and detector the system will experience anisoplanatism losses in the antenna gain of the adaptive optics laser transmitter. With a synchronous equatorial orbit satellite positioned near the zenith, and with a 1.6 m diameter laser transmitter telescope operating at a laser wavelength of 5000 \AA , we estimate that the ratio of the turbulence limited antenna gain, to the anisoplanatism limited antenna gain, to the diffraction limited antenna gain is as 1 : 120.5 : 589.7. The effect of anisoplanatism would be to reduce the antenna gain relative to the diffraction limit by a factor of 4.9—which is a significant amount, but not so much that a meaningful experiment couldn't be performed. We use the term "turbulence limited" to imply that there is no adaptive optics or high speed pointing correction involved in the transmitter operation, and that the telescope diameter is large compared to r_0 .

If we wished to be able to work even closer to the diffraction limit the laser transmitter could be operated at about $10,000 \text{ \AA}$. In this case the ratio of the turbulence limited antenna gain, to the anisoplanatism limited antenna gain, to the diffraction limited antenna gain will be as 1 : 74.2 : 111.7. Here the effect of anisoplanatism is to reduce the antenna gain relative to the diffraction limited by a factor of only 1.5—which is so near to unity that we can virtually consider the anisoplanatism effect to be nonexistent. Needing to choose a wavelength different from the SLC operational wavelength is of little consequence. What we want to accomplish with this experiment is to confirm the absence of surprises and the closer the expected performance is to diffraction limited the more certainly we can conclude that no surprises were encountered.

* For a synchronous orbit the required separation is about 800 m, while for a rather low orbit, namely 300 km altitude, the required separation is about 15 m. In either case a physical link to maintain the separation appears to be impractical—certainly it does not suggest a low cost for the satellite.

Co-locating the beacon and the laser detector eliminates one of the two things that made the satellite system so expensive, i. e. , it removes the station keeping requirement. But the beacon itself can impose a very severe cost penalty. Beacon pointing precision has to be of the order of a fraction of an arc second rms if the beacon is to be able to use the type of antenna gain that is needed to project sufficient power density from a synchronous equatorial orbit to the adaptive optics' wavefront distortion sensor on the ground. To eliminate the requirement for very fine pointing precision and for a stabilized spacecraft we have considered use of a corner reflector spacecraft with a ground based illuminator. An assembly of eight corner reflectors will provide a high gain return with virtually no cross-section variability with orientation.* This will allow use of a totally unstabilized satellite as far as the beacon function is concerned. In order to allow for the velocity aberration effect (which is what produces the so called point ahead requirement at the laser transmitter) it will be necessary to position the ground based illuminator for the corner reflectors "downstream" from the adaptive optics laser transmitter, so that the beacon return from the corner reflector will fall on the adaptive optics laser transmitter. The downstream distance would be the same as the nominally required station keeping distance between beacon and laser detector satellites, as discussed previously.

The same corner reflector arrangement could also serve to return a sample of the laser beam sent by the adaptive optics laser transmitter back to the ground. The intensity of this return would be directly proportional to the achieved adaptive optics antenna gain, so that no receiver/detector capability is required on the satellite. This allows us to entirely eliminate

* We assume that the corner reflectors are hollow, three front surface mirror assemblies. If the corner reflectors are of the prism type then there can be simultaneous return from two corner reflectors, and orientation dependent interferences which can make the cross-section variable.

the need for spacecraft stabilization and assures us of a low cost satellite, simple enough to be designed, fabricated, and tested in a short time. The schedule for deployment into space may, however, be a much longer term matter.

In examining the concept of this type of beacon we have noticed a potential problem with beacon signal strength. For a corner reflector satellite in a synchronous equatorial orbit if we used a 0.05 m diameter ground based illuminator operating at 5000 Å, illumination wavelength, so that the illuminator operation would be nearly ideal, i. e. diffraction limited, despite turbulence effects, then with a 0.3 m diameter corner reflector the illuminator power would have to be about 100 watts to provide sufficient beacon power to the adaptive optics' wavefront distortion sensor. While not impossible, the size of the diffraction limited corner reflectors and the power at the illuminator are both inconveniently large. Moreover, the beacon illuminator would have to be located about 800 m downstream from the adaptive optics laser transmitter unit—an inconvenient operational consideration. We believe that the concept we have just described could be used as the basis for an experiment to verify that there are no surprises introduced into the performance of a high gain adaptive optics laser transmitter by the need to project a nearly collimated beam through the upper atmosphere. However, while this configuration certainly appears to be considerably cheaper to deploy than the two satellite concepts we originally described we have also considered a low orbit version of the corner reflector satellite as an even simpler and cheaper option. As a sample of a low orbit system we consider a corner reflector satellite in a 1000 km altitude circular orbit. Periodically this satellite will pass almost directly overhead of the adaptive optics laser transmitter, and for a period of up to 80 seconds that it can spend within 15° of the zenith, the laser transmitter experiment can be performed. At this altitude we can get sufficient beacon power to the

adaptive optics wavefront distortion sensor with the illuminator power reduced to about one watt and with corner reflectors of about 0.025 m diameter. In this case the satellite is trivially simple, the ground based illuminator is a rather modest unit, and the downstream displacement of the illuminator relative to the adaptive optics laser transmitter is only about 50 m, which operationally is a conveniently small distance.*

The one serious objection to the use of a satellite at this low altitude is that because of its lower altitude, it has a greater velocity, and consequently the point ahead angle will be greater. In this case it is nearly 50 μ rad, compared to about 20 μ rad for a synchronous equatorial orbit. As a consequence the anisoplanatism effect will be much more severe. For operation at 5000 \AA , laser wavelength the 1.6 m diameter laser transmitter would have a ratio of the turbulence limit to the anisoplanatism limit to the diffraction limit for the antenna gain of 1:10.5:590. Clearly in this case anisoplanatism so limits the antenna gain that very little could be proven about how well adaptive optics performs in sending a nearly collimated beam up through the atmosphere. If, however, we consider operating the laser transmitter at 10,000 \AA wavelength then the ratio of turbulence limited to anisoplanatism limited to diffraction limited antenna gain is as 1:30.7:112. In this case the effect of anisoplanatism is to only reduce the antenna gain by a factor of 3.6 relative to its diffraction limited value. Operating the adaptive optics transmitter at a laser wavelength of 10,000 \AA we should be able to develop fairly conclusive evidence that there are no surprises introduced by the need to transmit a nearly collimated beam through the upper atmosphere.

* If the satellite altitude were 500 km rather than a 1000 km then the downstream displacement would be only 25 m, but for this altitude the time spent within 15° of the zenith would be only about 40 seconds.

Since the corner reflector will serve as both the beacon and the laser detector equipment in space, and since with an array of eight corner reflectors the unit will operate quite satisfactorily no matter what its orientation, we are potentially dealing with the simplest kind of satellite, unstabilized and entirely passive. This does however, leave open the question of how to acquire the satellite in the first place. To allow for satellite acquisition without giving up the simplicity of an unstabilized passive unit we suggest a satellite design based on a "sheet metal" array of eight large radar corner reflectors, each corner perhaps one meter in diameter. * No matter what the orientation the radar cross-section would be very large so that there would be no problem achieving radar acquisition. To facilitate handover to an optical tracker the "sheet metal" would be painted diffuse white so that the satellite would have a large scattered sunshine signature. The positioning of the optical corner reflectors in the satellite would be quite simple. To avoid any shadowing of the optical corner reflectors by the radar corner reflector, the eight optical corner reflectors would be located, one at the bottom (i. e. the vertex) of each of the eight radar corner reflectors. †

With the satellite concept thus defined we are now ready to provide some numerical analysis results. This is taken up in the next section for both the satellite experiment and the aircraft experiment.

* For a satellite positioned in a synchronous equatorial orbit it might be desirable to make the size of the radar corner reflectors several meters in diameter. Exact size would depend on an examination of the capabilities of the available acquisition radars.

† The possibility that this satellite could be shared with another DARPA program should be explored.

2.4 Numerical Considerations

In the preceding discussion we have at various points made allusion to practical quantitative constraints. In this section we shall present the analysis and calculations defining the magnitude of these constraints. For convenience, we shall divide our presentation into four subsections treating propagation effects, point-ahead geometry, signal-to-noise ratio considerations for the aircraft experiment, and signal-to-noise ratio considerations for the satellite experiment.

2.4.1 Propagation Effects

The theory governing optical propagation through atmospheric turbulence is quite well established and accordingly, it will be sufficient for us to simply quote the relevant results here. We are potentially interested in four quantities. These are the effective coherence diameter, r_0 , the Greenwood frequency, f_0 , the isoplanic patch size, ϑ_0 , and the log-amplitude variance, σ_L^2 . The physical significance of the effective coherence diameter, r_0 , is quite well known. It governs the size of the adaptive optics elements in as much as it results in a loss in antenna gain if the element size is much greater than r_0 . The loss in antenna gain due to element size, d , is approximately as

$$\eta_{LS} = \exp\left[-\left(\frac{d}{\alpha r_0}\right)^{5/3}\right], \quad (1)$$

where α is a constant with a value between unity and 3.4, the exact value of which depends on the interelement influence function for the adaptive optics corrector. While the diffraction limited antenna gain for an aperture of diameter D operating at wavelength λ is given by the expression

$$G_{DL} = \frac{1}{4} \pi (D/\lambda)^2, \quad (2)$$

the corresponding turbulence limited antenna gain (in the absence of any adaptive optics correction, and assuming a very large physical diameter for the aperture) is given by the expression

$$G_{TL} = \frac{1}{4} \pi (r_0 / \lambda)^2, \quad (3)$$

The value of the effective coherence diameter, r_0 , is given by the expression

$$r_0 = \left\{ 0.423 k^2 \int_{\text{PATH}} ds C_N^2 (s/L)^{5/3} \right\}^{-3/5}, \quad (4)$$

for propagation of a point source over a path of total length L , with the point source located at $s=0$ and the value of r_0 evaluated at $s=L$. This value of r_0 applies for a laser transmitter located at $s=L$ transmitting a beam focused at $s=0$. The quantity k denotes the optical wave number, i. e.,

$$k = 2\pi / \lambda, \quad (5)$$

where λ is the wavelength of interest. The notation C_N^2 denotes the refractive-index structure constant, a geophysical quantity defining the optical strength of atmospheric turbulence, a quantity whose value can vary along the propagation path. Using the estimated value for C_N^2 as given in Eq. (6), i. e.,

$$C_N^2 = \begin{cases} 8.4 \times 10^{-15} (h/18.5)^{-2}, & 18.5 < h < 110 \\ 2.5 \times 10^{-15}, & 110 < h < 1500 \\ 8.87 \times 10^{-15} (h/1000)^{-3}, & 1500 < h < 7000 \\ 6.34 \times 10^{-15} (h/1000)^{-\frac{1}{2}}, & 7000 < h < 20500 \\ 0, & 20500 < h, \end{cases} \quad (6)$$

as applying to the AMOS site, where h is altitude above the facility, we have carried out calculations of the effective coherence diameter, r_0 , for various

aircraft heights, H , and ground ranges, R . The slant path, which is the propagation path length, \mathcal{L} , is given by the expression

$$\mathcal{L} = (R^2 + H^2)^{1/2} \quad . \quad (7)$$

The point source was assumed to be located on the aircraft. Accordingly, the variable of integration, s , has zero value at the aircraft altitude, H , and is equal to the path length, \mathcal{L} , at the AMOS facility altitude, zero. This means that at the position along the propagation path defined by s , the altitude above the AMOS facility is given by the expression

$$h = H \left[1 - (s/\mathcal{L}) \right] \quad . \quad (8)$$

Our results for the value of r_0 , for a wavelength $\lambda = 5.0 \times 10^{-7}$ m, are shown in Fig. 3 for aircraft altitudes from 2.5 km to 20.0 km above the AMOS facility altitude, for ground ranges out to 30 km. It is apparent from these results that we can explore the effect of different values of r_0 in the range of 0.15 m to 0.05 m by working at an altitude of $H=2.5$ km above the AMOS facility, at ground ranges from zero to about 15 km. Though if we wish, and other considerations do not prevent it, we can work at any of the other altitudes and ranges up to 30 km except that at 5 km altitude we almost certainly would not want to work at a ground range beyond 20 km.

The Greenwood frequency, f_0 , provides a basis for estimation of the servo bandwidth that the adaptive optics control system must have. If the servo bandwidth is actually f_s , then the rms residual wavefront error associated with servo lag in the adaptive optics system will be

$$\sigma_{sl}^2 = (f_0/f_s)^{5/3} \quad , \quad (9)$$

and so long as the servo lag is not too great then the antenna gain of the adaptive optics will be reduced by the servo lag efficiency factor

$$\eta_{sl} = \exp(-\sigma_{sl}^2) \quad . \quad (10)$$

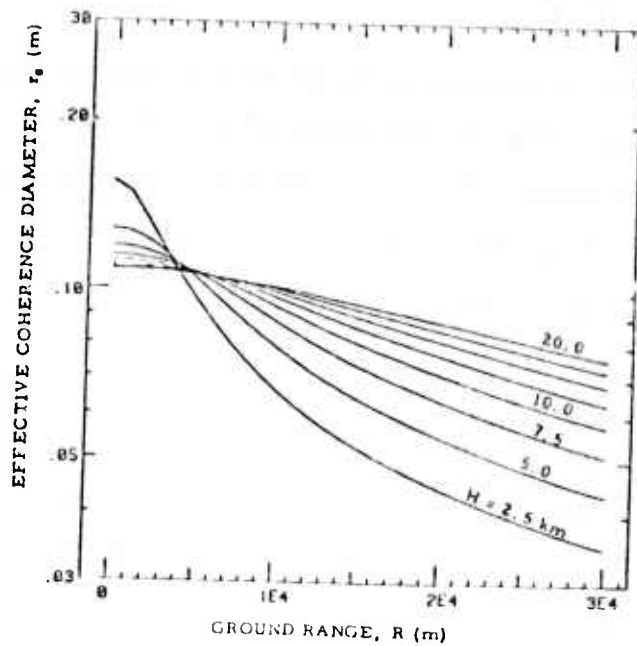


Figure 3. Effective Coherence Diameter.

Results are shown for a 5.0×10^{-7} m wavelength point source at an altitude H . The value of the effective coherence diameter, r_e , is determined at the ground end of the propagation path.

The Greenwood frequency, f_0 , for a point source can be evaluated using the equation

$$f_0 = \left\{ 0.102 k \int_{\text{PATH}} ds C_N^2 V^{5/3} \left(\frac{s}{L} \right)^{3/5} \right\}^{3/5}, \quad (11)$$

where the propagation integral involves the same dependencies here as in Eq. (4). The point source is considered to be located at the $s=0$ end of the propagation path while the adaptive optics aperture for which the Greenwood frequency applies is located at the other end, where $s=L$. The quantity V in Eq. (11) denotes the perpendicular component of the velocity of the air relative to the propagation path. It can be written as

$$V = \omega (L - s) + V_w, \quad (12)$$

where V_w is the ambient wind velocity* and can be approximated by the expression

$$V_w = \begin{cases} |1.03 - 3.47 \times 10^{-3} (h + 3000)|, & h < 9600, \\ |-103.97 + 4.87 \times 10^{-3} (h + 3000)|, & h > 9600. \end{cases} \quad (13)$$

The quantity ω in Eq. (12) denotes the angular rate of the line-of-sight so that ω (rad-s) defines the velocity with which the line-of-sight is "dragged" through the atmosphere. This angular rate is determined by the aircraft velocity, V_A , according to the equation

$$\omega = V_A / L \quad (14)$$

Using an assumed aircraft velocity of $V_A = 200$ m/sec we have evaluated the Greenwood frequency, f_0 , for the same range of conditions as previously considered for the evaluation of r_0 . These results are shown Fig. 4, and are

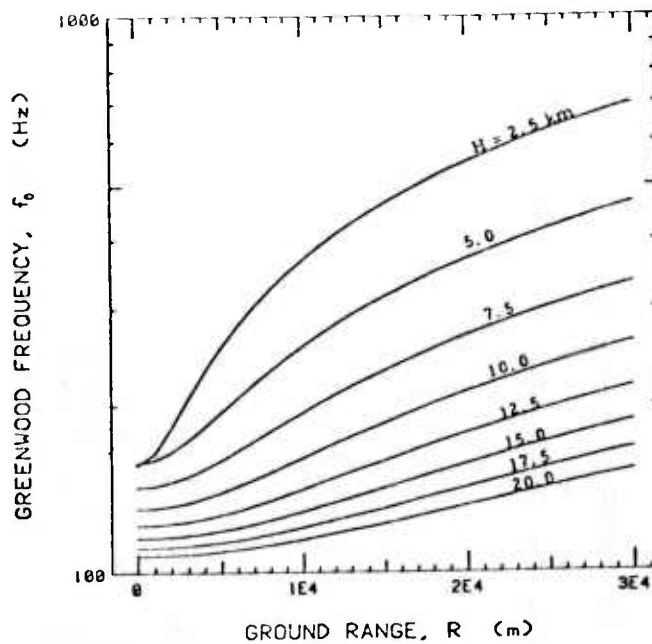


Figure 4. Greenwood Frequency.

Results shown here correspond to the same range of conditions apply to Fig. 3.

* We make the worst case assumption that the ambient wind direction is perpendicular to the propagation path.

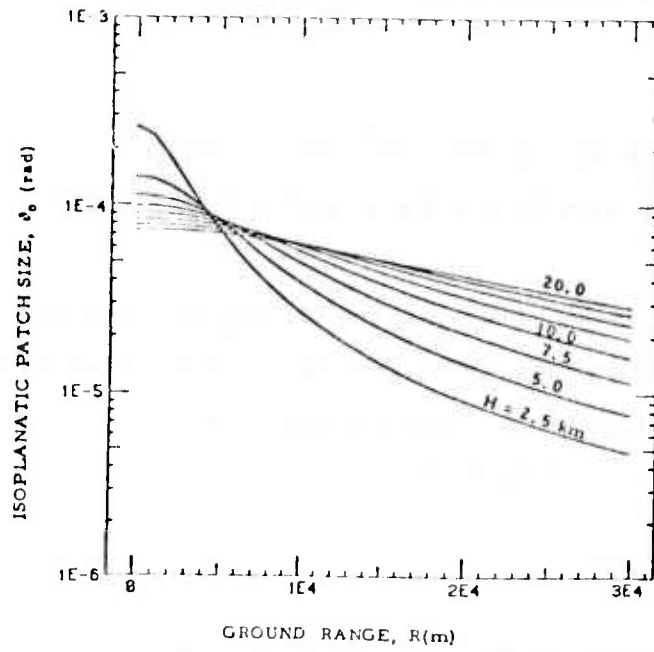


Figure 5. Angular Extent of the Isoplantic Patch.

Results shown here correspond to the same range of conditions applying to Fig. 3.

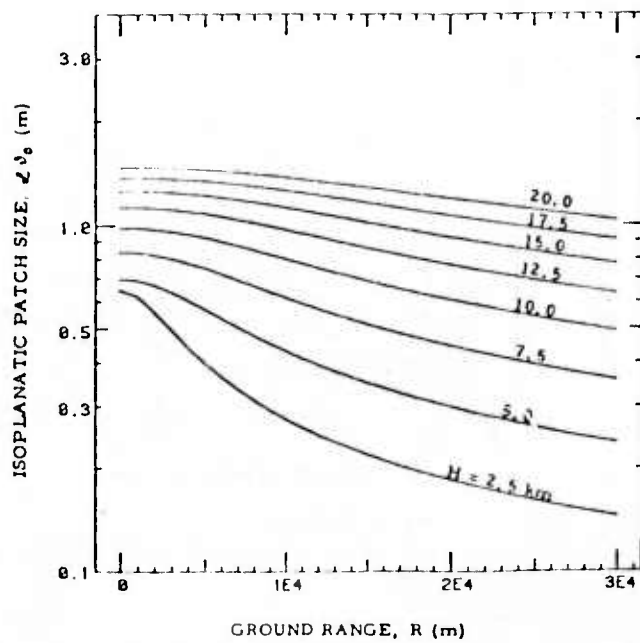


Figure 6. Linear Extent of the Isoplantic Patch.

Results shown here correspond to the same range of conditions applying to Fig. 3.

to be understood as defining the required servo bandwidth for an adaptive optics system at the AMOS facility transmitting a laser beam focused at the aircraft. Actually, of course, the required servo bandwidth will be greater than the Greenwood frequency by a factor of three to five. This is required so that the servo lag induced loss in antenna gain will be small, i. e., of the order of a few percent. Examining Fig. 4 it is obvious that for all cases of interest a servo bandwidth of the order of $f_s = 1500$ Hz should be more than adequate for all aircraft experiments.

The isoplanatic patch size, ϑ_0 , defines the field-of-view size for the adaptive optics transmitter beyond which the required wavefront corrections are significantly different. For the transmitted laser beam focused on the aircraft the isoplanatic patch size is given by the expression

$$\vartheta_0 = \{0.423 k^2 \int ds C_N^2 (s/L)^{5/3} (L-s)^{5/3}\}^{-3/5} \quad (15)$$

This quantity has been evaluated for a 5000 Å wavelength laser transmitter for the same set of aircraft altitudes and ground ranges as were treated for Fig. 3. The results are shown in Fig. 5. Of somewhat greater direct significance is the linear extent of the isoplanatic patch, given by the quantity $L \vartheta_0$. This quantity is plotted in Fig. 6. As can be seen from Fig. 6 the linear extent of the isoplanatic patch is in all cases less than about 1.5 m, and generally less than 1.0 m. This means that if the aircraft mounted pod is long enough to allow the separation between the beacon and the detector to be varied over a 2.0 m range, then we will have the ability to explore the full range of anisoplanatism effects.

The last of the propagation effects of concern to us relates to intensity fluctuations/random apodization. This matter which principally concerns the need for random apodization "correction" of the adaptive optics transmitter is perhaps best measured in terms of the log-amplitude variance, σ_L^2 , to be associated with the beacon radiation as observed at the adaptive optics transmitter aperture, assuming that the beacon wavelength is the

same as that of the laser transmitter. In this case the value of the log-amplitude variance, σ_{ℓ}^2 , is given by the expression

$$\sigma_{\ell}^2 = 0.56 k^{7/8} \int ds C_N^2 (s/L)^{5/6} (L-s)^{5/6} . \quad (16)$$

The fundamental effect of the log-amplitude variance, σ_{ℓ}^2 , upon the performance of the adaptive optics laser transmitter is to reduce the antenna gain by a factor of

$$\eta_{RA} = \exp(-\sigma_{\ell}^2) , \quad (17)$$

due to a lack of a random apodization capability in the adaptive mechanism. As a practical matter this effect will be just barely perceptible unless the log-amplitude variance is greater than 0.1 nepers².

In Fig. 7 we show values for the log-amplitude variance calculated for the same laser wavelength, $\lambda = 5000 \text{ \AA}$, and set of aircraft altitudes and ground ranges treated in Fig. 3. As can be seen from an inspection of Fig. 3, it is possible to find combinations of aircraft altitude and ground range for which the log-amplitude variances will be significantly greater than 0.1 nepers². However, on referring to Fig. 3 we can see that these conditions imply values of the effective coherence diameter, r_0 , which are much less than 0.07 m. Thus it appears that the largest value of σ_{ℓ}^2 that can be achieved will be about 0.1 nepers². This implies that we will just barely, if at all, be able to observe the effect of random apodization on adaptive optics laser transmitter antenna gain.

For transmission to a satellite in a synchronous equatorial orbit or in a circular orbit at 1000 km altitude essentially the same propagation equations apply, except that Eq. (14) for the apparent angular velocity, ω , has to be revised. For the synchronous equatorial orbit

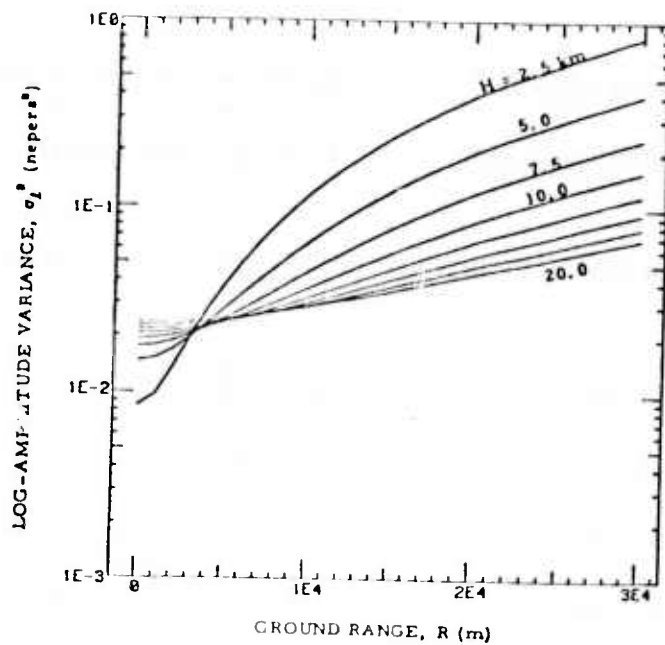


Figure 7. Log-Amplitude Variance.

Results shown here correspond to the same range of conditions applying to Fig. 3.

$$\omega = 0 \text{ rad/sec, (synchronous orbit) ,} \quad (14a)$$

while for the 1000 km altitude orbit

$$\omega = 6.91 \times 10^{-3} \text{ rad/sec, (1000 km altitude orbit) .} \quad (14b)$$

Using these values together with the preceding equations we have calculated that for operation at a laser wavelength of $5000 \overset{\circ}{\text{A}}$

$$r_0 = \begin{cases} 0.1007 \text{ m} & \text{(1000 km altitude orbit)} \\ 0.1006 \text{ m} & \text{(synchronous orbit)} \end{cases} , \quad (18)$$

$$f_0 = \begin{cases} 122.6 \text{ Hz} & \text{(1000 km altitude orbit)} \\ 60.2 \text{ Hz} & \text{(synchronous orbit)} \end{cases} , \quad (19)$$

$$\sigma_l^2 = \begin{cases} 0.0297 \text{ nepers}^2 & \text{(1000 km altitude orbit)} \\ 0.0298 \text{ nepers}^2 & \text{(synchronous orbit)} \end{cases}, \quad (20)$$

For operation at a laser wavelength of $10,000 \overset{\circ}{\text{A}}$ the corresponding results are

$$r_0 = \begin{cases} 0.231 \text{ m} & \text{(1000 km altitude orbit)} \\ 0.231 \text{ m} & \text{(synchronous orbit)} \end{cases}, \quad (21)$$

$$f_0 = \begin{cases} 53.4 \text{ Hz} & \text{(1000 km altitude orbit)} \\ 26.2 \text{ Hz} & \text{(synchronous orbit)} \end{cases}, \quad (22)$$

$$\sigma_l^2 = \begin{cases} 0.0132 \text{ nepers}^2 & \text{(1000 km altitude orbit)} \\ 0.0133 \text{ nepers}^2 & \text{(synchronous orbit)} \end{cases}, \quad (23)$$

The calculation of anisoplanatism effects for finite aperture sizes which is the matter of real interest to us here is considerably more complicated than is implied by the simplicity of Eq. (15). The value of the isoplanatic patch size for operation at a laser wavelength of $5000 \overset{\circ}{\text{A}}$ is

$$\vartheta_0 = 10.35 \mu\text{rad}, \quad (24)$$

and for a $10,000 \overset{\circ}{\text{A}}$ laser wavelength it is

$$\vartheta_0 = 23.8 \mu\text{rad}. \quad (25)$$

While for very large aperture diameters the effect of anisoplanatism with a point-ahead angle of ϑ is to reduce the antenna gain by a factor of $\exp[-(\vartheta/\vartheta_0)^{5/3}]$, for a more modest sized antenna the actual effect of anisoplanatism on antenna gain is too complex in its derivation to be presented here. The theory for this, along with sample values, is developed in our internal

report, TR-249*. We find that for modest sized antenna diameters point-ahead angles as great or greater than ϑ_0 can be tolerated. It is these results rather than the value of ϑ_0 per se that governed our thinking in formulating the satellite experiment.

This completes our quantitative consideration of atmospheric turbulence propagation effects. In the next section we shall consider matters related to point-ahead geometry.

* D. L. Fried, "Isoplanatism Dependence of a Ground-to-Space Laser Transmitter with Adaptive Optics," the Optical Sciences Company Report No. TR-249, March 1977.

2.4.2 Point Ahead

The basic point-ahead problem is that as measured in an inertial frame of reference, by the time the light from a laser transmitter reaches the vicinity of what was the location of the beacon at the time the beacon sent out the photons the detection of which is being used to control the transmitter's orientation—by that time the beacon has moved to a new position. Thus if the transmitted laser radiation is to reach the beacon, the transmitter must not be pointed at where the beacon appears to be, i. e. , at where it was, but must be pointed ahead of where the beacon appears to be, i. e. , to where it will be. This is the point ahead requirement.

The one-way time of flight of the light is

$$\tau = R/C$$

where R is the range and $C = 3 \times 10^8$ m/sec is the speed of light. If the velocity of the beacon relative to the transmitter, as measured in an inertial frame of reference* is V then in a round-trip time, 2τ , the beacon will have moved a distance $2\tau V$. It is this distance that the point ahead angle, ϑ , must accommodate. We can write

$$\vartheta = 2\tau V/R \quad , \quad (27)$$

from which it follows that

$$\vartheta = 2V/c \quad . \quad (28)$$

For the aircraft experiment the beacons' relative velocity is

* It is important to recall that the rotating earth does not constitute an inertial frame of reference. Hence, a satellite in an synchronous equatorial orbit, though it seems to have no relative velocity, actually has a significant relative velocity in an inertial frame of reference.

nominally $V = 200$ m/sec so that the required point-ahead angle $\vartheta = 1.33 \times 10^{-6}$ rad. This is small enough that we can consider it to be virtually negligible.* For a satellite in a circular orbit at altitude H the velocity is

$$V_s = 1.996 \times 10^7 (R_E + H)^{-1/2} \quad , \quad (29)$$

where $R_E = 6.378 \times 10^6$ m is the (nominal) radius of the earth. The velocity of a ground station at the AMOS facility (due to rotation of the earth) is approximately $V_{AMOS} = 4.337 \times 10^2$ m/sec. Consequently the relative velocity between the AMOS Facility and a satellite at an altitude of $H = 1.0 \times 10^6$ m will be

$$V = V_s \pm V_{AMOS} \quad , \quad (30)$$

where $V_s = 7.348 \times 10^3$ and the plus or the minus sign is used accordingly as the satellite moves about the earth contrary to or in the same sense as the earth's rotation. Assuming that the two velocities are in the same sense, so that the minus sign applies, then the relative velocity will be $V = 6.914 \times 10^3$ m/sec for a satellite in a 1000 km altitude circular orbit. In this case the point ahead angle is $\vartheta = 46.1 \times 10^{-6}$ rad, and the point ahead linear distance is $H\vartheta = 46.1$ m.

For a satellite in a synchronous equatorial orbit, for which $R_E + H \approx 4 \times 10^7$ m, satellite velocity is $V_s = 3.157 \times 10^3$ m/sec. In this case the relative velocity will be $V = 2.72 \times 10^3$ m/sec, and the point-

* It is perhaps interesting to note that if the laser transmitter had absolute boresight control, with $\lambda/D = 5 \times 10^{-7} / 1.6 = 3.125 \times 10^{-7}$ rad, the laser beam main lobe would miss the beacon by almost 4 beam widths unless point-ahead were allowed for. But without absolute boresight control, and using a round-trip adaptive boresight adjustment we will not even be able to observe this small a point-ahead requirement.

ahead angle will be $\vartheta = 18.15 \times 10^{-6}$ rad. The point-ahead linear distance will be $H\vartheta = 610$ m.

A particularly significant feature of the point-ahead phenomena concerns the behavior of a corner reflector returned beam. If we insist on it, we could consider the corner reflector in the satellite to be moving relative to the ground facility and then calculate the Fitzgerald contraction (special relativity) induced "distortion" of the corner reflector, and accordingly calculate where the "retro directed" beam will actually go. It is, however, considerably simpler and equally valid (since all inertial frames are equivalent) to consider the corner reflector to be standing still and the ground to be moving with respect to it. Viewed in this manner and recognizing that the corner reflector will return the laser illuminator in the direction it came from, i. e., back to where the illuminator was when it sent out the laser radiation—but in the period of the round-trip transit time the illuminator's velocity relative to the corner reflector will have caused it to move one point-ahead distance. The corner reflector return will entirely miss the illuminator position, and if it is to be incident on the adaptive optics laser transmitter's aperture the laser illuminator must be displaced relative to the transmitter by one point-ahead length. This is just the quantity $H\vartheta$ evaluated above. For a corner reflector in a synchronous equatorial orbit its value is 610 m, and this is the distance that would have to exist between the beacon illuminator and the laser transmitter. Moreover, if the corner reflector return of the adaptive optics laser transmission is to be monitored for antenna gain evaluation, the receiver for that would have to be located 610 m on the other side of the adaptive optics laser transmitter. For the corner reflector satellite in a 1000 km altitude circular orbit the same situation applies, i. e., the beacon illuminator on one side of and the antenna gain monitoring receiver on the other side of the adaptive optics laser transmitter, but in this case the separations on each side would be only 16 m.

2.4.3 Beacon Power

In assessing the adequacy of the beacon as a reference that the adaptive optics wavefront distortion sensor can use we can use either of two criteria. We can simply determine the apparent stellar magnitude of the beacon as seen by the wavefront sensor, or we can ask how many photons the beacon delivers to an r_0 sized region of the transmitter aperture during a servo control bandwidth period. For the aircraft experiment it will be more convenient to use the former as a basis for evaluation.

For the aircraft experiment we contemplate use of a 200 W super high pressure mercury lamp.* This lamp produces about 10^4 lumens, with an intensity $I = 10^3$ lumens/steradian in all directions except those "blocked" by the pole pieces. The major dimension of the arc is $l = 2.2 \times 10^{-3}$ m. At a range of $R = 20 \text{ km} \equiv 2 \times 10^4$ m the lamp will produce a flux density of

$$\begin{aligned} E &= I/R^2 \\ &= 10^3 / (2 \times 10^4)^2 \\ &= 2.5 \times 10^{-6} \text{ lux} \end{aligned} \quad (31)$$

The corresponding stellar magnitude is

$$\begin{aligned} M &= 2.5 \log_{10} \left(\frac{E}{2.65 \times 10^{-6}} \right) \\ &= 0.06 \end{aligned} \quad (32)$$

or essentially a zero magnitude. We further note that at this range the $D = 1.6$ m diameter telescope operating at a nominal wavelength of $\lambda = 0.55 \times 10^{-6}$ m will have a resolution spot size of

* USHIO Corp., Lamp type USH-200D, or equivalent

$$\begin{aligned}
\delta &= R (\lambda/D) \\
&= 2 \times 10^4 (0.55 \times 10^{-6} / 1.6) \\
&= 6.88 \times 10^{-3} \text{ m}
\end{aligned}
\tag{33}$$

This means that the telescope can not resolve the beacon, so that we can consider the beacon to constitute a single resolution element. Accordingly, we can classify the beacon as having a brightness equivalent to zero magnitude per resolution element* at a range of 20 km. Going out to 30 km the brightness will fall about one stellar magnitude. At 10 km range the beacon will remain unresolved and its apparent brightness will increase by about 1.5 stellar magnitudes.

Apparently there will be little or no difficulty in getting a sufficiently bright beacon for the aircraft experiment, since the Compensated Imaging System can work adequately with a ninth magnitude per resolution element reference and can work very well with a sixth magnitude per resolution element reference. Accordingly, a zero magnitude per resolution element beacon should provide a more than adequate † reference source for control of the adaptive optics in the aircraft experiment.

We start our analysis of the satellite experiment by considering the case (rejected in our experiment planning because of implementation problems) of a laser transmitter onboard the satellite. For a beacon laser wavelength, λ , and an onboard transmitter diameter, d , if the transmitted power is, P , then at range, R , the beacon power density would be

$$\theta = P \left[\frac{1}{4} \pi (d/\lambda)^2 \right] R^{-2}
\tag{34}$$

* This does not make any allowance for atmospheric transmission losses, which may cost us several stellar magnitudes.

† With 100:1 attenuation through the atmosphere this would still be a fifth magnitude per resolution element reference.

For an adaptive optics subelement (center-to-center) spacing, r , with a photodetection quantum, η , during a time τ there will be

$$N = \frac{1}{4}\pi r^2 \theta \eta \tau / \delta , \quad (35)$$

photons detected, where

$$\begin{aligned} \delta &= hc/\lambda , \\ &= 2 \times 10^{-25} / \lambda , \end{aligned} \quad (36)$$

is the energy per photon. The effective signal-to-noise voltage ratio, SNR_v , available to control the adaptive optics is

$$SNR_v = N^{1/2} . \quad (37)$$

Reasonable values for the various parameters are as follows:

$$\begin{aligned} \lambda &= 6.33 \times 10^{-7} \text{ m} \\ d &= 0.1 \text{ m} \\ P &= 1.0 \times 10^{-3} \text{ W} \\ R &= 4.0 \times 10^7 \text{ m} \end{aligned}$$

so that

$$\theta = 1.225 \times 10^{-8} \text{ W/m}^2 , \quad (38)$$

and

$$\delta = 3.160 \times 10^{-19} \text{ J/photon} . \quad (39)$$

With

$$\begin{aligned} r &= 0.1 \text{ m} \\ \eta &= 0.1 \\ \tau &= 1.0 \times 10^{-3} \text{ sec.} \end{aligned}$$

we get

$$N = 3.04 \times 10^4 \text{ detections,} \quad (40)$$

and

$$\text{SNR}_v = 1.74 \times 10^2 \quad . \quad (41)$$

This is a more than adequate signal-to-noise ratio.

Unfortunately, for practical reasons we had to drop the concept of a beacon laser transmitter and turn to consideration of a corner reflector in the satellite and a ground based illuminator. If the illuminator has a diameter d_i and transmits a power P_i , then the power density of the satellite will be

$$\theta_i = P_i \left[\frac{1}{2} \pi (d_i / \lambda)^2 \right] R^{-2} \quad . \quad (42)$$

If the corner reflector has an effective diameter d_{CR} then the power it will collect will be

$$P_{CR} = \frac{1}{4} \pi d_{CR}^2 \theta_i \quad . \quad (43)$$

The power density projected back to the adaptive optics by the diffraction limited spread of the corner reflector will be

$$\theta = P_{CR} \left[\frac{1}{4} \pi (d_{CR} / \lambda)^2 \right] R^{-2} \quad (44)$$

Eq. 's (35) and (37) then apply just as written.

For the synchronous orbit satellite we consider the following set of parametric values;

$$\lambda = 5.0 \times 10^{-7} \text{ m}$$

$$d_i = 0.03 \text{ m}$$

$$R = 4.0 \times 10^7 \text{ m}$$

$$d_{cR} = 0.3 \text{ m}$$

$$P_i = 100 \text{ W}$$

so that

$$\delta = 4.0 \times 10^{-19} \text{ J/photon,} \quad (45)$$

$$\theta_i = 1.767 \times 10^{-4} \text{ W/m}^2, \quad (46)$$

$$P_{cR} = 1.249 \times 10^{-5} \text{ W,} \quad (47)$$

and

$$\theta = 2.21 \times 10^{-9} \text{ W/m.} \quad (48)$$

Just as before using the wavefront distortion sensor parameter values of

$$r = 0.1 \text{ m}$$

$$\eta = 0.1$$

$$\tau = 1.0 \times 10^{-3} \text{ sec.}$$

we get

$$N = 4.33 \times 10^3 \text{ detections,} \quad (49)$$

and

$$\text{SNR}_v = 65.8 \quad (50)$$

This is clearly also a quite adequate signal-to-noise ratio. In fact, it is sufficiently large that we might be able to reduce the illuminator power from 100 watts to 10 watts (thereby reducing the signal-to-noise voltage ratio to $SNR_v = 20.8$), or reduce the corner reflector diameter from 30 cm to about 16.5 cm (thereby reducing the signal-to-noise voltage ratio to $SNR_v = 19.9$). Either reduction might be tolerated but not both, and in fact with either our design margin is getting rather slim.

When we consider the 1000 km altitude circular orbit then the relevant propagation parameters are as follows:

$$\lambda = 5.0 \times 10^{-7} \text{ m}$$

$$d_i = 0.03 \text{ m}$$

$$R = 1.0 \times 10^6 \text{ m}$$

$$d_{cR} = 0.025 \text{ m}$$

$$P_i = 1.0 \text{ W}$$

so that

$$\mathcal{E} = 4.0 \times 10^{-19} \text{ J/photon} , \quad (51)$$

$$\theta_i = 2.827 \times 10^{-3} \text{ W/m}^2 , \quad (52)$$

$$P_{cR} = 1.388 \times 10^{-6} \text{ W} , \quad (53)$$

and

$$\theta = 2.725 \times 10^{-9} \text{ W/m}^2 . \quad (54)$$

Here again we use the wavefront distortion sensor parameters of

$$r = 0.1 \text{ m}$$

$$\eta = 0.1$$

$$\tau = 1.0 \times 10^{-3} \text{ sec}$$

so that we get

$$N = 5.35 \times 10^3 \text{ detections} \quad , \quad (55)$$

and

$$\text{SNR}_v = 73.2 \quad . \quad (56)$$

This is a clearly an entirely adequate signal-to-noise ratio and allows us quite adequate design margin, with some rather nonstressing design parameters. We have concluded that this represents a preferred design approach for the beacon.

2.5 Conclusions and Summary for Chapter II

The preceding sections have reviewed the various considerations associated with an UpLink transmitter demonstration, and have presented sample designs (in an overview sense), along with some supporting analysis. Subject to the constraint of a short term relatively low cost program we have configured a two part demonstration/experiment utilizing an adaptation of the Compensated Imaging System on the AMOS 1.6 m diameter telescope as the adaptive optics laser transmitter. The first part of the experiment, which will allow testing of all aspects of the UpLink adaptive optics theory except for the propagation of a nearly collimated beam through the upper atmosphere relies on an aircraft carrying a beacon and laser detector. A simple arrangement for measuring antenna gain, by switching transmitter diameter and observing the effect of the laser detector has been described. A high pressure, 200 watt, mercury lamp is shown to provide an adequately bright beacon reference at 20 to 30 km range, with no pointing requirement — so that the special aircraft equipment for the experiment should be remarkably simple. It appears reasonable to expect the aircraft experiment to start producing results within 18 to 24 months.

The second part of the experiment would address only the additional effects that might be encountered when we send a nearly collimated laser beam through the upper atmosphere. It is based on a very simple, unstablized and entirely passive satellite, in a nominally 1000 km altitude circular orbit. The satellite would consist of set of eight large (i. e., about one meter diameter) radar corner reflectors assembled so as to cover all the octants of the sphere, and painted white so as to have a reasonably sized reflected sunlight signature. Eight optical (mirror) corner reflectors, each one inch in diameter would be placed in the satellite, one at the vertex of each of the eight radar corner reflectors. A one watt, three centimeter diameter, 5000 Å laser wavelength ground based illuminator would be located 46 meters from the AMOS telescope. It would

illuminate the satellite so that the corner reflector return would be available at the telescope as the beacon reference. A small telescope located 46 meters on the other side of the AMOS telescope would collect the UpLink laser transmission intercepted and returned by the corner reflector. From the measurement results provided by this small telescope it would be possible to determine the adaptive optics antenna gain.

In the aircraft experiment the adaptive optics laser transmitter would send a laser beam whose wavelength was near 5000 \AA , i. e., in the blue-green. However, for the satellite experiment, to keep the anisoplanatism effect to a tolerable level, the wavelength of the laser beam transmitted by the adaptive optics would be near $10,000 \text{ \AA}$.

We believe that the combination of the aircraft experiment with the satellite experiment will allow us to demonstrate the basic UpLink technology, and will allow us to address all of the questions relevant to our understanding of the operation of UpLink adaptive optics. Moreover, we believe that a program configured along these lines would be relatively inexpensive and could be producing results within a relatively short time.

addresses	number	line
	of copies	number
Donald Hanson RADC/DUSE	10	
RADC/CA GRIFFISS AFB NY 13441	1	1
RADC/TSLD GRIFFISS AFB NY 13441	1	2
RADC/DAP GRIFFISS AFB NY 13441	2	3
ADMINISTRATOR DEF TECH INF CTR ATTN: DTIC-JDA CAMERON SIA BG 5 ALEXANDRIA VA 22314	12	5
Optical Sciences Company PO Box 446 Placentia, California 92670 ATTN: Dr. David L. Frie	5	2
Space Division P.O. Box 92960 worldways Postal Center Los Angeles, CA 90009 Attn: INCS/Maj G. Lamparter	1	3
Space Division P.O. Box 92960 worldways Postal Center Los Angeles, CA 90009 ATTN: INCS Capt. Jackson	1	4
Space Division P.O. Box 92960 worldways Postal Center Los Angeles, CA 90009 Attn: TCD	1	5
HQ ADCOM Peterson AFB, CO 80914 Attn: INAY	1	6

ARRDSD The Pentagon Washington, DC 20301 Attn: Maj H. Stears	1	7
ODDR&C The Pentagon Washington, DC 20301 Attn: Mr. J. Brockway	1	8
AF/SASC The Pentagon Washington, DC 20301 Attn: Capt James Hengle	1	9
ARPA/SIO 1400 Wilson Blvd Arlington, VA 22209 Attn: Lt Col A. Herzberg	1	10
ARPA/SIO 1400 Wilson Blvd Arlington, VA 22209 Attn: Dr. C. Thomas	1	11
ARPA/DEO 1400 Wilson Blvd Arlington, VA 22209 Attn: LCDR W. Wright	1	12
Office of Naval Research 490 Summer Street Boston, MA 02110 Attn: Dr. Fred Quelle	3	13
AFDL/OP Hanscom AFB, MA 01731 Attn: Dr. John Garing	1	14
AFSL/ALO Kirtland AFB, NM 81117 Attn: Dr. C. B. Hogge	1	15
AFSC/DL Andrews AFB, DC 20334 Attn: Capt Doble	1	16
AFSC/RRFD Andrews AFB, DC 20334	1	17

JS Army Advanced Ballistic Missile Agency Huntsville Office P.O. Box 1500 Huntsville, AL 35807 Attn: Mr. W. Davies	1	18
RLD Wright Patterson AFB, OH 45433 Attn: Supt/Mr. C. Chapin	2	19
RADC (DL-A3) c/o AVCO Everett Research Labs P.O. Box 251 Puhanua, Maui, HI 96704 Attn: Capt Gary Danlen	1	20
Aerospace Corp. P.O. Box 92957 Los Angeles, CA 90009 Attn: Mr. Yura	1	21
Aerospace Corp. P.O. Box 92957 Los Angeles, CA 90009 Attn: Mr. Michelson	1	22
Aerospace Corp. P.O. Box 92957 Los Angeles, CA 90009 Attn: Mr. Turner	1	23
AVCO Everett P.O. Box 251 Puhanua, HI 96704 Attn: Program Manager	2	24
Hughes Aircraft Co. Cantinsola & Teale Sts Denver City, CA 90230 Attn: John F. Heintz	1	25
Institute for Defense Analyses 400 Army Navy Dr Arlington, VA 22202 Attn: Dr. I. Wolfhard	1	26
Visibility Lab University of California La Jolla, CA 92037 Attn: Mr. J. McElmery	1	27
ITT Corp. 10 Maguire Road Levinston, VA 02173 Attn: Mr. Paul Mailhot	3	28

DMSAIC-0 P.O. Box 1500 Huntsville, AL 35807 Attn: W. J. Lavan	1	29
Hughes Research Labs 3011 Malibu Canyon Road Malibu, CA 90265 Attn: Dr. Tom O'Meara	1	30
Perkin Elmer Corp. Main Avenue Norwalk, CT 06850 Attn: Dr. R. Hufnagel-270	1	31
Riverside Research Institute 60 West End Avenue New York, NY 10023 Attn: Dr. Marvin King	2	32
AVCO Everett Research Lab 2350 Revere Beach Pkwy Everett, MA 02149 Attn: Mr. P. Howes	1	33
Charles Stark Draper Lab 195 Albany Street Cambridge, MA 02139 Attn: Dr. Keto Soosaar	2	34
MIT/Lincoln Lab P.O. Box 73 Lexington, MA 02173 Attn: Dr. V. Reis	2	35
HQ ADCOM Peterson AFB, CO 80914 Attn: XPDI	1	36
HQ ADCOM Peterson AFB, CO 80914 Attn: XPDS	1	37
FTD Wright Patterson AFB, OH 45433 Attn: Mr. A. I. Larson	2	38
Hughes Research Labs 3011 Malibu Canyon Road Malibu, CA 90265 Attn: Dr. W. Brown	1	39

ml/Lincoln Lab P.O. Box 73 Lexington, MA 02173 Attn: Dr. J. Greenwood	1	40
Naval Ocean Systems Center Code 3105 San Diego, CA 92152 Attn: Mr. L. Stotts	2	41
University of California, Santa Barbara Department of Physics Santa Barbara, CA 93106 Attn: Dr. Harold W. Lewis	1	42
NOAA Environmental Research Lab Wave Propagation Lab R45x1 Boulder, CO 80302 Attn: Mr. Robert S. Lawrence	1	43
NOAA Environmental Research Lab Wave Propagation Lab R45x1 Boulder, CO 80302 Attn: Mr. J. Ochs	1	44
Pacific Sierra Research Corp. 1456 Clover Field Street Santa Monica, CA 90404 Attn: Dr. Richard Lutomirski	1	45
Ohio State University Electro Science Lab 1320 Sinear Road Columbus, OH 43212 Attn: Dr. Stuart A. Collins	1	46
Naval Postgraduate School Dept of Mechanical Engineering Code 59 HA Monterey, CA 93940 Attn: Dr. Thomas. W. Hoolihan	1	47